Research Paper

GEOSPHERE

GEOSPHERE

https://doi.org/10.1130/GES02908.1

12 figures; 4 supplemental files

CORRESPONDENCE: jakecovault@gmail.com, jake.covault@beg.utexas.edu

CITATION: Covault, J.A., Sylvester, Z., and Dunlap, D.B., 2026, Landslide influence on delta stratigraphy, northeastern Gulf of Mexico: Geosphere, https://doi.org/10.1130/GES02908.1.

Science Editor: David E. Fastovsky
Associate Editor: Andrea Fildani

Received 11 July 2025
Revision received 2 December 2025
Accepted 12 December 2025

Published online 9 January 2026

Landslide influence on delta stratigraphy, northeastern Gulf of Mexico

Jacob A. Covault, Zoltán Sylvester, and Dallas B. Dunlap

Bureau of Economic Geology, Jackson School of Geosciences, The University of Texas at Austin, Austin, Texas 78758, USA

ABSTRACT

Although wave, tide, and river controls on deltas are well established, there has been less work on the influence of growth faults and submarine landslides on delta stratigraphy and deep-water sediment delivery. We used an ~1200 km² portion of a three-dimensional seismic-reflection dataset (wherein peak frequency ranges ~30 Hz to 50 Hz in the shallow interval) in the northeastern Gulf of Mexico[1] to document the stratigraphic evolution of its shelf margin during the last 0.5 m.y. We mapped five deltas, which were deposited one at a time during glacio-eustatic lowstands since oxygen isotope stage (OIS) 14. Deltas active during OIS 12, 10, and 6 are erosionally truncated by submarine landslides, which nucleated along prominent growth faults. The landslide-dominated interval shows progressively increasing thickness variability in deposits filling local landslide scarps. In addition, depocenters migrated great distances, ~10 km on average, but with a lot of variability from one delta to the next (5–20 km). Prominent submarine channels formed in the landslide scarps, and downstream mass-transport deposits constrained channel orientation. Shelf-margin evolution is different along strike in the east, where the older, well-documented Fuji-Einstein delta complex lacks landslides and exhibits more typical geometries of unperturbed deltas, i.e., lenticular cross-sectional and oval map-view geometries, with submarine channels forming in prodelta gullies rather than landslide scarps. Our detailed mapping and analysis of shelf-margin evolution in the northeastern Gulf of Mexico during the last half million years are useful as a process analog for older, poorly imaged, and/or locally sampled subsurface intervals there and in other settings with delta-fed submarine channels.

INTRODUCTION

Deposition at river mouths creates deltas, which are significant sinks for sediment and organic carbon burial (Hage et al., 2022; Haq and Milliman, 2023). Deltas play an important role in coastal morphology (Nienhuis et al., 2020) and form much of the stratigraphy of continental margins (Allen, 2017). During sea-level lowstands, shelf-edge deltas on passive margins, such as the northeastern Gulf of Mexico, are staging areas for terrigenous sediment delivery to the deep sea through submarine channels (Fig. 1).

The deposits of subsurface deltas can be hydrocarbon source beds and reservoirs (Wright, 1985; Meckel, 2003), and they are the focus of recent exploration efforts for carbon storage in the Gulf of Mexico (Meckel et al., 2017). Subsurface delta stratigraphic architecture typically comprises clinoforms as a result of seaward progradation (Fig. 2; Berg, 1982; Winker and Edwards, 1983; Suter and Berryhill, 1985; Sylvester et al., 2012; Paumard et al., 2020). Small-scale (i.e., several to tens of square meters in area) physical experiments have provided insights into delta evolution related to sea-level change (e.g., Martin et al., 2009; Straub, 2019), and computational approaches have been used to produce 3-D stratigraphy of field-scale (hundreds of square kilometers in area) river- and wave-dominated deltas for reservoir-analog and coastal impact studies (e.g., Falivene et al., 2019; Willis and Sun, 2019; Willis et al., 2021; Hariharan et al., 2022).

However, the influence of structures such as growth faults and submarine landslides, common in "unstable" shelf margins (Coleman et al., 1983; Winker and Edwards, 1983), on delta stratigraphy is less clear. Intuitively, fault offsets and landslide scarps should disrupt the clinoform stratigraphy typical of deltas, and we aimed to explore the following less understood aspects of deltas in unstable margins:

(1) Compensational stacking, i.e., preferential deposition in topographic lows adjacent to previous deposits (Straub et al., 2009), is considered to be the quintessential autogenic sedimentary process governing delta evolution. How does compensational stacking proceed when faults and landslides introduce roughness elements to the seafloor of the margin?

(2) Recent physical experiments of basin filling have used various measures to show a decrease in sedimentation variability during longer time scales (Sheets et al., 2002; Straub et al., 2009). This has been attributed to local deposition and negligible subsidence during shorter time scales, but more broadly distributed deposition across an entire subsiding basin during longer time scales (Straub et al., 2009). These experiments are from alluvial basins and shelf margins lacking the submarine landslide and channel-formation processes of full-scale systems (Sheets et al., 2002; Strong and Paola, 2008; Martin et al., 2009; Sylvester et al., 2024).

[1]The Gulf of Mexico was renamed to the Gulf of America in the United States in 2025 by the U.S. Department of the Interior, but retained its original name internationally and during the writing of this work. It appears as the Gulf of Mexico throughout this publication, following the naming standards for international bodies of water set by the International Hydrographic Organization.

Jacob Covault https://orcid.org/0000-0002-7907-0516

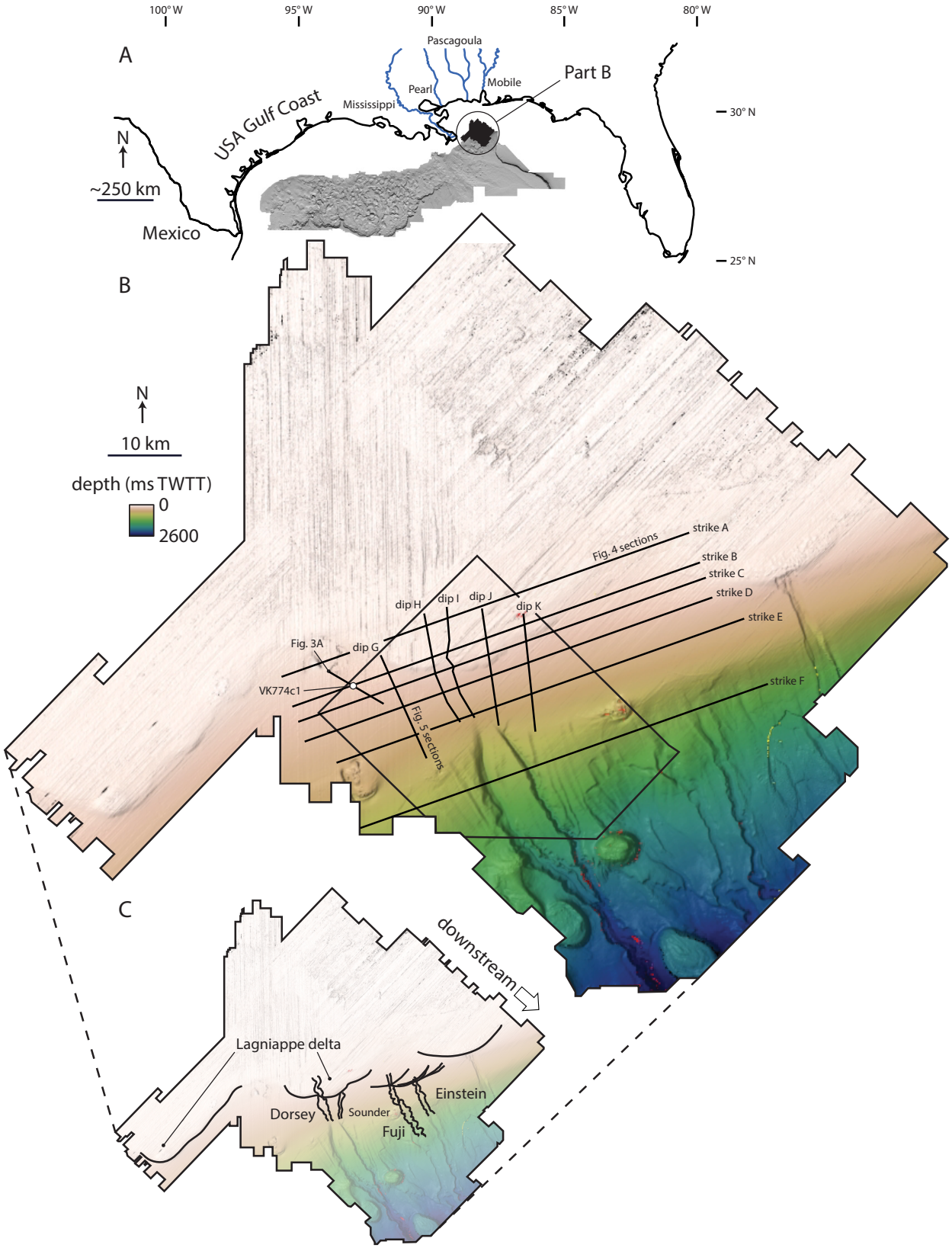

Figure 1. Study area location map. (A) U.S. Gulf Coast including rivers of potential importance in delivering sediment to northeastern Gulf of Mexico. Footprint of part B seismic-reflection volume B-32c-93-LA is encircled black polygon (Supplemental File S1 [see text footnote 2]). Grayscale shaded relief map is from U.S. Bureau of Ocean Energy Management (https://www.boem.gov/oil-gas-energy/mapping-and-data/map-gallery/boem-northern-gulf-mexico-deepwater-bathymetry-grid-3d). (B) Seafloor of the seismic-reflection volume B-32c-93-LA. Locations of seismic-reflection profiles are indicated with black lines; footprint of area interest is approximately rectangular polygon. TWTT—two-way traveltime. (C) Locations of delta fronts and submarine channels modified from Sylvester et al. (2012).

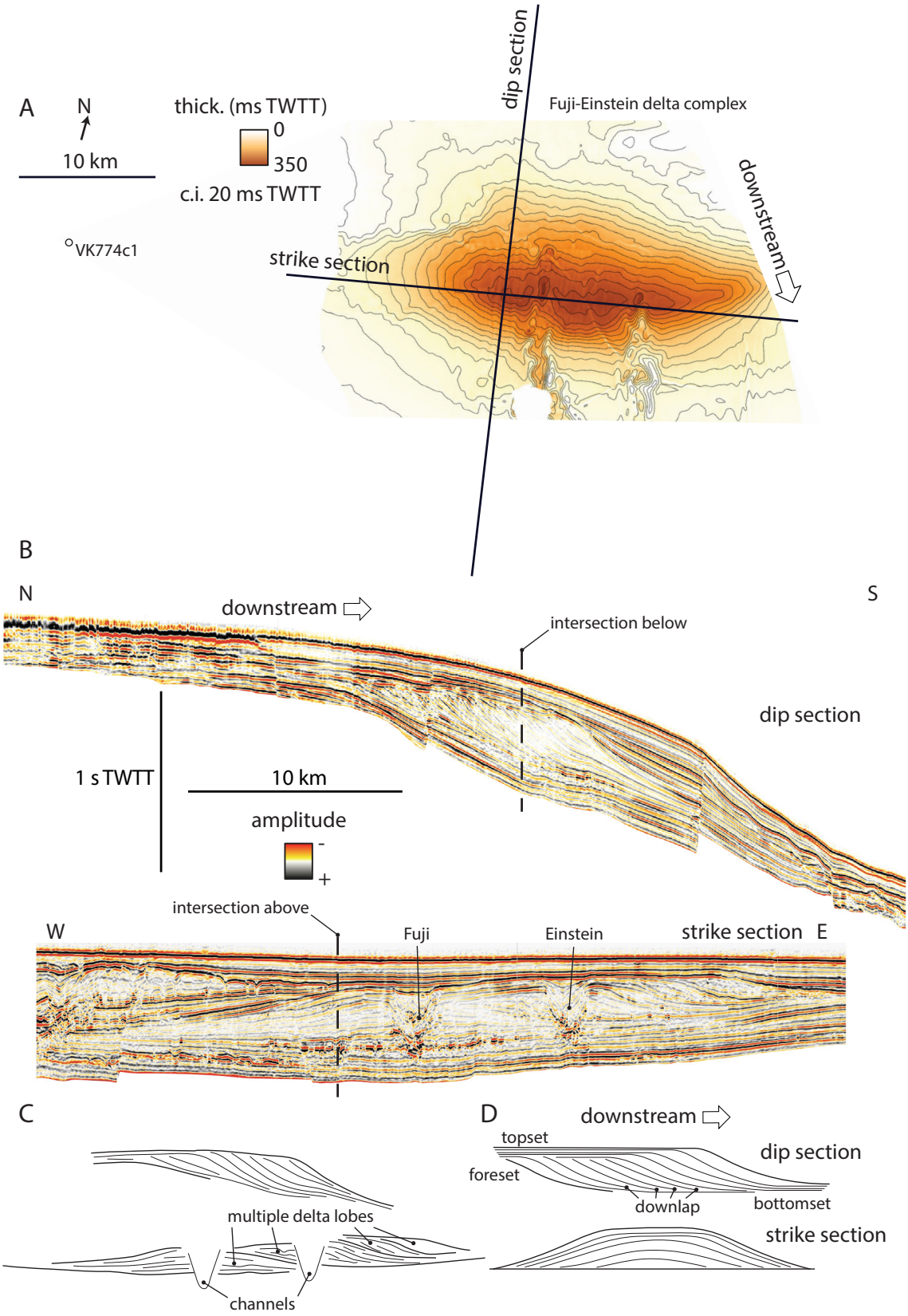

Figure 2. Typical shelf-edge delta morphology and stratigraphy. (A) Time thickness map of Fuji-Einstein delta complex from Sylvester et al. (2012). Top and bottom horizons used to generate this thickness map are shown most prominently in Figure 4. (B) Depositional strike and dip seismic-reflection profiles from Sylvester et al. (2012). (C) Line-drawing trace of profiles in B. "Multiple delta lobes" are compensationally stacked from left to right (west to east). (D) Example of typical delta strike and dip profiles from Berg (1982). TWTT—two-way traveltime; c.i.—contour interval.

How does basin filling evolve in unstable margins where these processes might recur?

(3) What is the origin of submarine channels in these settings? Do they form as a result of progressive widening of gullies sourced by deltas (e.g., Straub and Mohrig, 2009; Straub et al., 2012; Sylvester et al., 2012) or as a result of headward erosion of landslide scarps, especially in unstable shelf margins prone to failure (e.g., Farre et al., 1983; Pratson and Coakley, 1996)? What are the implications of these models for deep-water sediment delivery?

We used an ~1200 km^2 portion of a 3-D seismic-reflection dataset (~40 Hz dominant frequency in the shallow interval) in the northeastern Gulf of Mexico to document the stratigraphic evolution of its unstable shelf margin during the last 0.5 m.y. (Fig. 3; Fillon et al., 2004). From this stratigraphic framework, we interpreted the timing of deltas and submarine-channel formation at the shelf edge, where they were affected by landslides. This shelf-margin evolution is useful as a process analog for examining older subsurface intervals of the Gulf of Mexico (Hackbarth and Shew, 1994; Kendrick, 2000; Godo, 2006) and other settings with delta-fed submarine channels, such as the deep-water basins beyond the Nile, Magdalena, and Niger deltas (e.g., Winker and Edwards, 1983; Damuth, 1994; Romero-Otero et al., 2015). For example, the characteristics of Pleistocene submarine-channel systems in the shallow subsurface of the northeastern Gulf of Mexico have been used to better predict the heterogeneity of deeper oil and gas reservoirs there (Hackbarth and Shew, 1994; Clemenceau and Miller, 1993; Kendrick, 2000). Likewise, some of the well-imaged, thoroughly mapped Pleistocene deltas in this region, like those of Sylvester et al. (2012) and this study, can be used to inform carbon storage assessment of the Miocene interval in the northern Gulf of Mexico (e.g., Wallace et al., 2014). Moreover, understanding submarine landslide occurrence and its impact on sediment dispersal through channels also has implications for geohazard assessment in the Gulf of Mexico and other resource-rich basins (Kneller et al., 2016). That is, the delta-front landslides we analyzed for this study represent analogs for shelf-margin geohazards (Campbell, 1999). By understanding their formative processes and stratigraphic evolution, we can better account for their risk to underwater infrastructure.

GEOLOGIC SETTING

The passive continental margin offshore Mississippi and Alabama prograded >50 km into the northeastern Gulf of Mexico since the Miocene (Godo, 2006). This progradation formed a broad shelf with rapid subsidence at the shelf edge as a result of extensional gravity sliding of the continental slope (Fig. 1; Winker, 1982; Winker and Edwards, 1983). Sylvester et al. (2012) calculated the shelf-edge subsidence rate in this region to be ~0.6 mm/yr (see also Anderson and Fillon, 2004). Consequently, Miocene–late Pleistocene shelf-edge deltas were offset by growth faults with thick, hanging-wall deposits (Winker, 1982; Coleman et al., 1983). Movement along growth faults and associated landslides are geohazard risks of unstable, progradational clastic margins, like the Gulf of Mexico (Coleman et al., 1983; Winker and Edwards, 1983). Growth faults can promote landslides by oversteepening the seafloor and weakening the substrate along the fault plane. However, late Pleistocene deltas in the Gulf of Mexico have other characteristics that precondition slopes to fail and produce landslides: rapid sedimentation, such as might be expected in the hanging wall of a shelf-edge growth fault, interbedded high- and low-permeability strata that allow buildup of pore pressure, and weak, clay-rich layers (Hampton et al., 1996). For example, overlying large growth-fault systems at the front of the modern Mississippi delta, there are landslides and gullies across slopes <0.5° (Shepard, 1955; Prior and Suhayda, 1979; Coleman et al., 1983).

During glacio-eustatic lowstands of the last ~1 m.y., deltas of the Mobile River and, possibly, the Pascagoula River prograded to the shelf edge and delivered sediment to the Fuji, Einstein, Dorsey, and Sounder submarine channels (Figs. 1 and 3; Kindinger, 1989; Anderson et al., 2004; Fillon et al., 2004; Kohl et al., 2004; Roberts et al., 2004; Sylvester et al., 2012; Carter et al., 2016; Portnov et al., 2020). Glacio-eustatic lowstand periods are indicated by even-numbered oxygen isotope stage (OIS) phases with relatively large oxygen-18 isotope values measured in deep-sea core samples; warmer interglacial periods are indicated by odd-numbered OIS phases with smaller oxygen-18 isotope values (Lisiecki and Raymo, 2005). The focus of this study was the Dorsey-Sounder delta complex, named after the Dorsey and Sounder submarine channels. The Dorsey-Sounder delta complex was active beginning in OIS 13 (Fillon et al., 2004; Roberts et al., 2004). The Lagniappe delta overlies the Dorsey-Sounder delta complex; the Lagniappe delta was deposited in the region beginning in OIS 5 (Kindinger, 1989; Kolla et al., 2000; Roberts et al., 2004). Later, we discuss Dorsey-Sounder delta evolution relative to the nearby, older Fuji-Einstein delta complex. Hackbarth and Shew (1994) indicated the Einstein channel formed ca. 790 ka during OIS 20 (Fig. 3; see also Winker, 1993). The Einstein channel and its upstream delta deposits are compensationally stacked to the east atop Fuji deposits; together, these systems approximate an oval-shaped delta ~30 km in the east-west direction across the shelf edge (Fig. 2; Sylvester et al., 2012). The Fuji-Einstein delta complex thins downstream, to the south, from ~400 ms two-way traveltime (TWTT) at the shelf edge into deep water, where two channels extend across the slope (Figs. 1 and 2; Sylvester et al., 2012). Research wells penetrate the channel fill and western levee of the Einstein channel system; coarse sediment is restricted to relatively high-amplitude seismic reflections at the base of the Einstein channel system in ~60 Hz data (Hackbarth and Shew, 1994; Sylvester et al., 2012). Sylvester et al. (2012) mapped channel bases along trough reflections.

The Dorsey and Sounder channels and their deltas are stacked to the west of the Fuji and Einstein delta complex (Figs. 1 and 4). Gulf of Mexico Shelf-Slope Research Consortium (GOMSSRC) core VK774c1 indicates the deltas were deposited since OIS 14 (Kolla et al., 2003; Fillon et al., 2004; Roberts et al., 2004), which is approximately the depth of the Tromso horizon of Portnov et al. (2020; see also Fig. 3 herein). The deltas prograded to the shelf edge during sea-level falls and lowstands (Kolla et al., 2003; Fillon et al., 2004; Roberts et al., 2004). The GOMSSRC focused their research on the Lagniappe delta, and

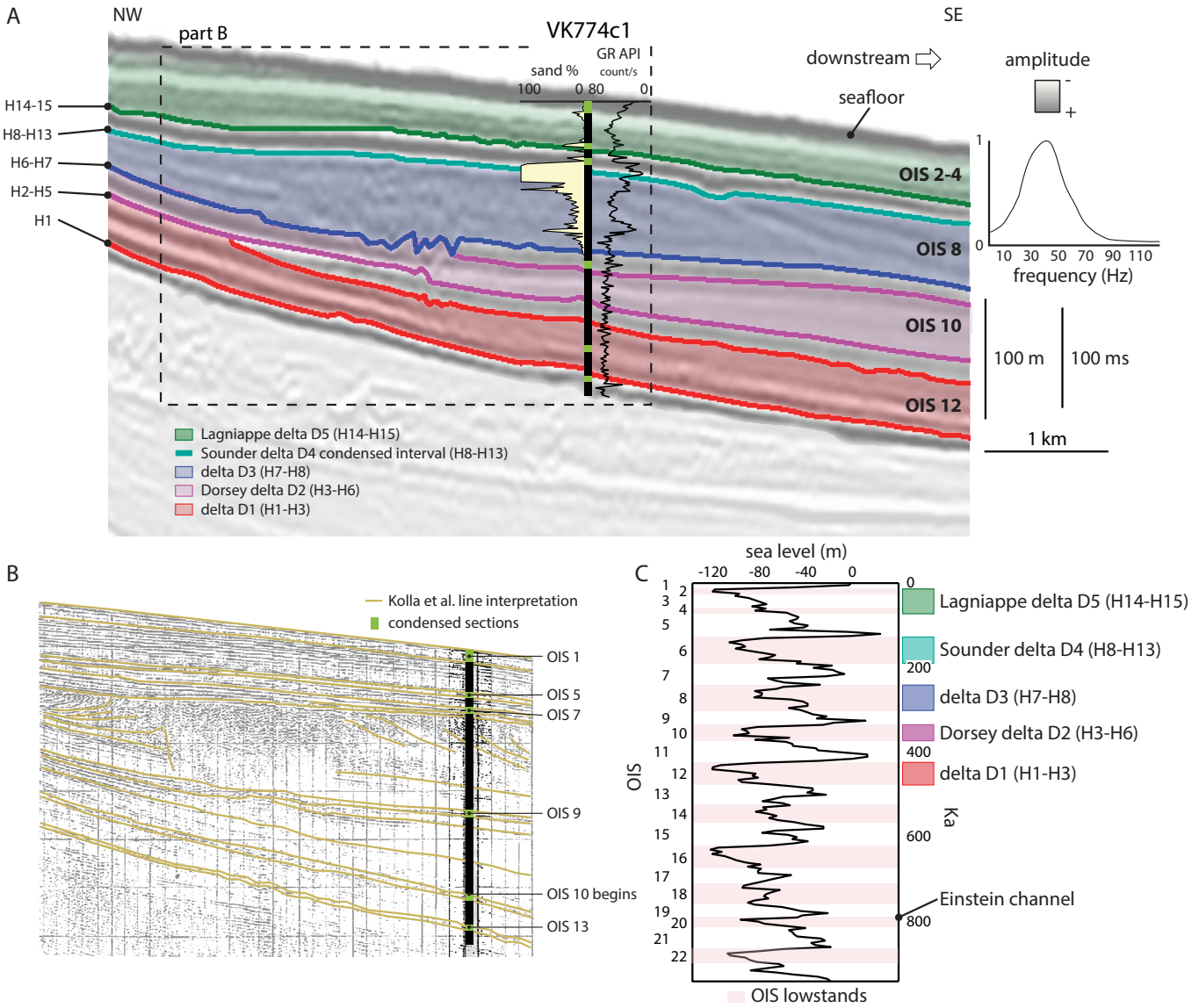

Figure 3. Age control for this study. (A) Seismic-reflection profile near VK774c1 core (location indicated with bold vertical black line). Small green polygons in VK774c1 are high-amplitude/parallel reflections in 1–2 m vertical resolution "boomer" profile from Kolla et al. (2003) shown in part B. These seismic facies are condensed sections deposited during oxygen isotope stage (OIS) highstands (Kolla et al., 2003; see also Fillon et al., 2004; Roberts et al., 2004). Sand % and gamma-ray (GR) logs are from Roberts et al. (2004). (B) Higher-resolution "boomer" profile from Kolla et al. (2003; see also Sydow and Roberts, 1994; Kolla et al., 2000). (C) Sea level of Miller et al. (2011) and oxygen isotope stages (OIS) of Lisiecki and Raymo (2005) relative to deltas of this study.

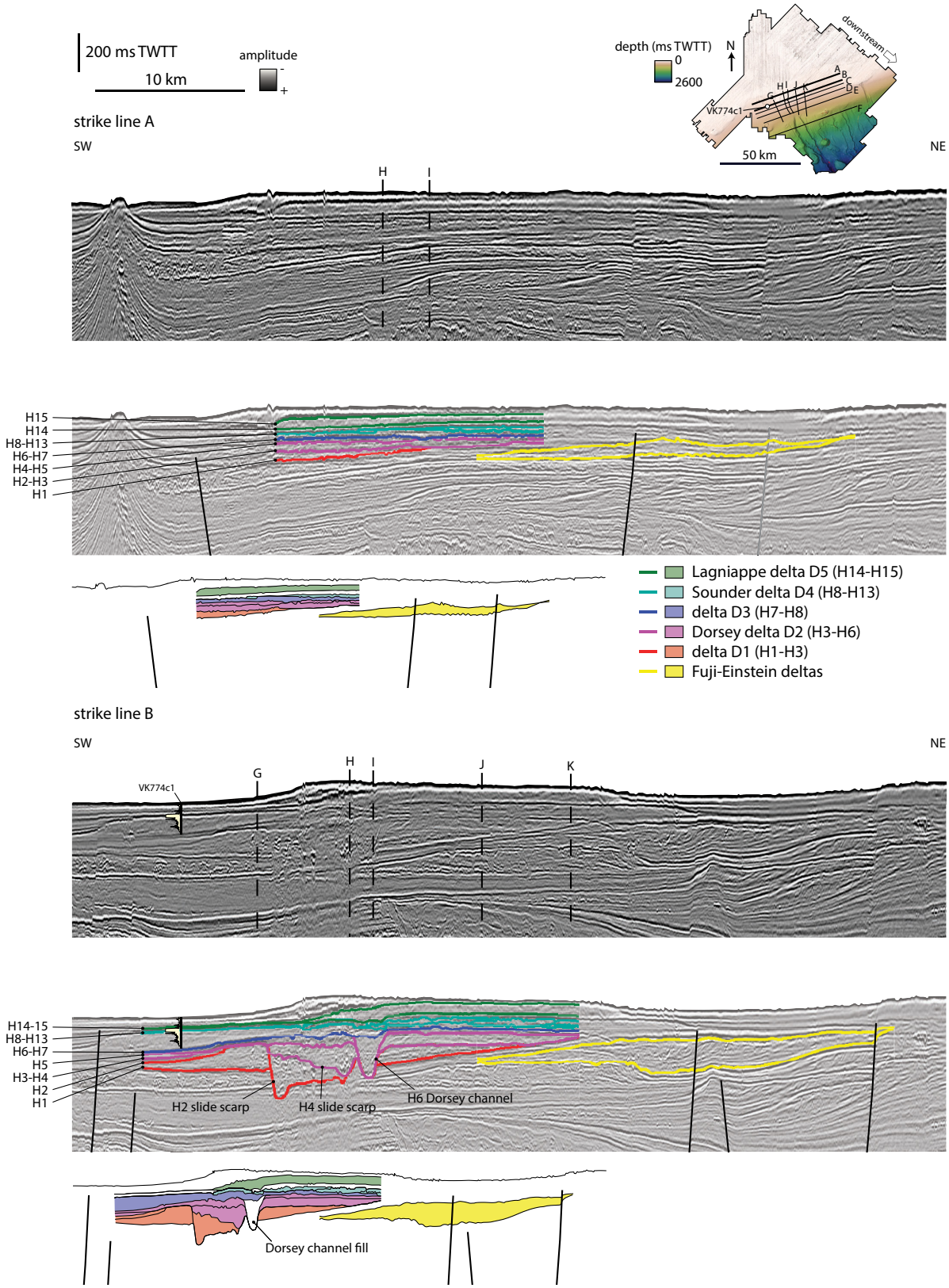

Figure 4. Depositional-strike profiles arranged from proximal to distal: profiles A–F. The Dorsey and Sounder channels formed after the Dorsey delta D2 and Sounder delta D4, respectively, reached the shelf edge; the channels are younger than the underlying deltas they incised. Because deltas thin from axis to margin, their multiple bounding and internal horizons can appear to merge into a single reflection at their margins. Where this occurs, the overlapping horizons are labeled (e.g., H14–H15) instead of a single horizon (e.g., H15). Steeply dipping black lines of interpreted profiles are faults. Prominent shelf-edge growth fault is indicated by bold black lines in profiles C, D, and E. See Figure 6, H1and H9, for map trace of this fault. See Figure 1 for profile locations. See also Supplemental File S3 (text footnote 2). TWTT—two-way traveltime. (*Continued on following two pages.*)

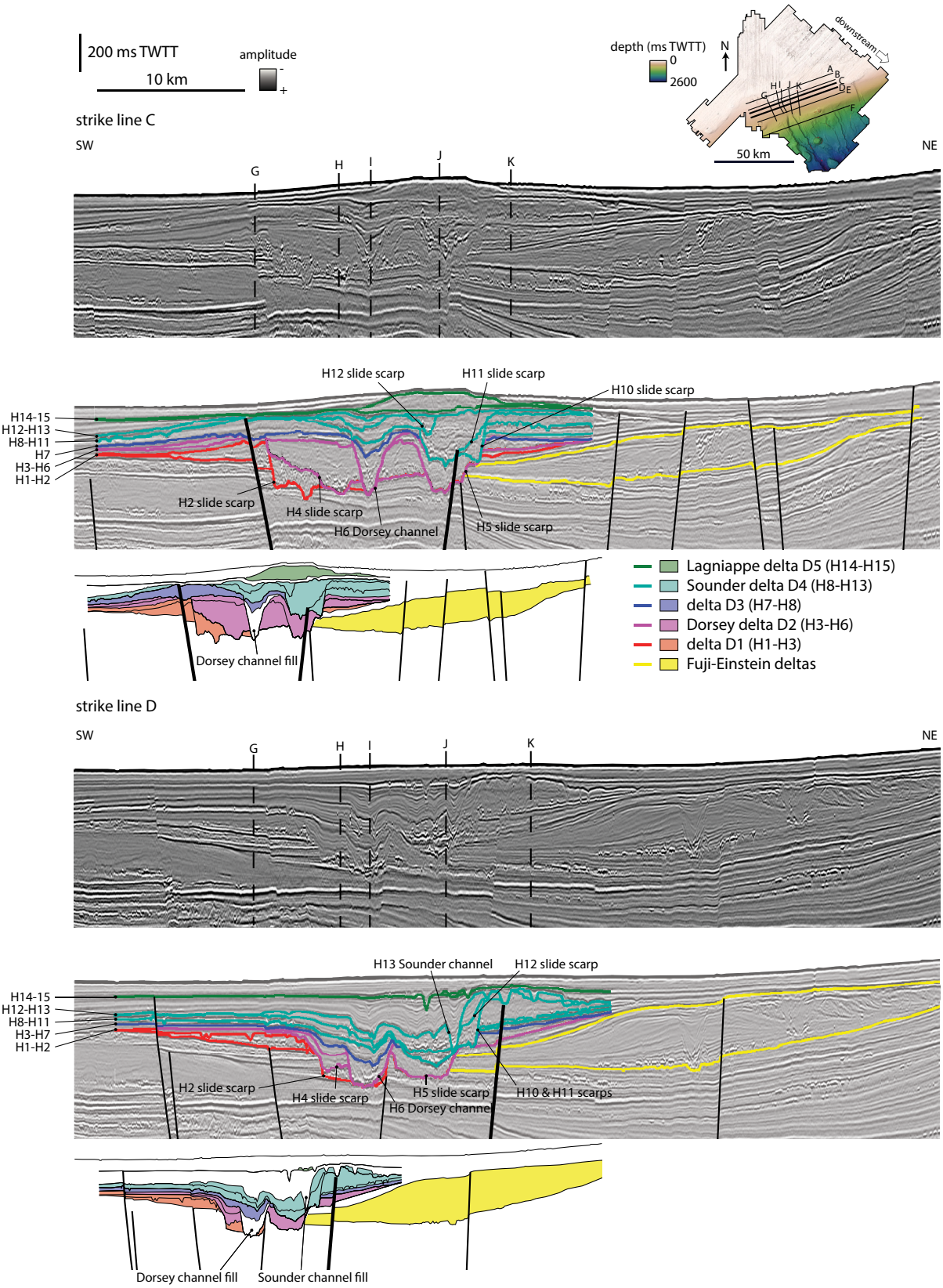

Figure 4 (*continued*).

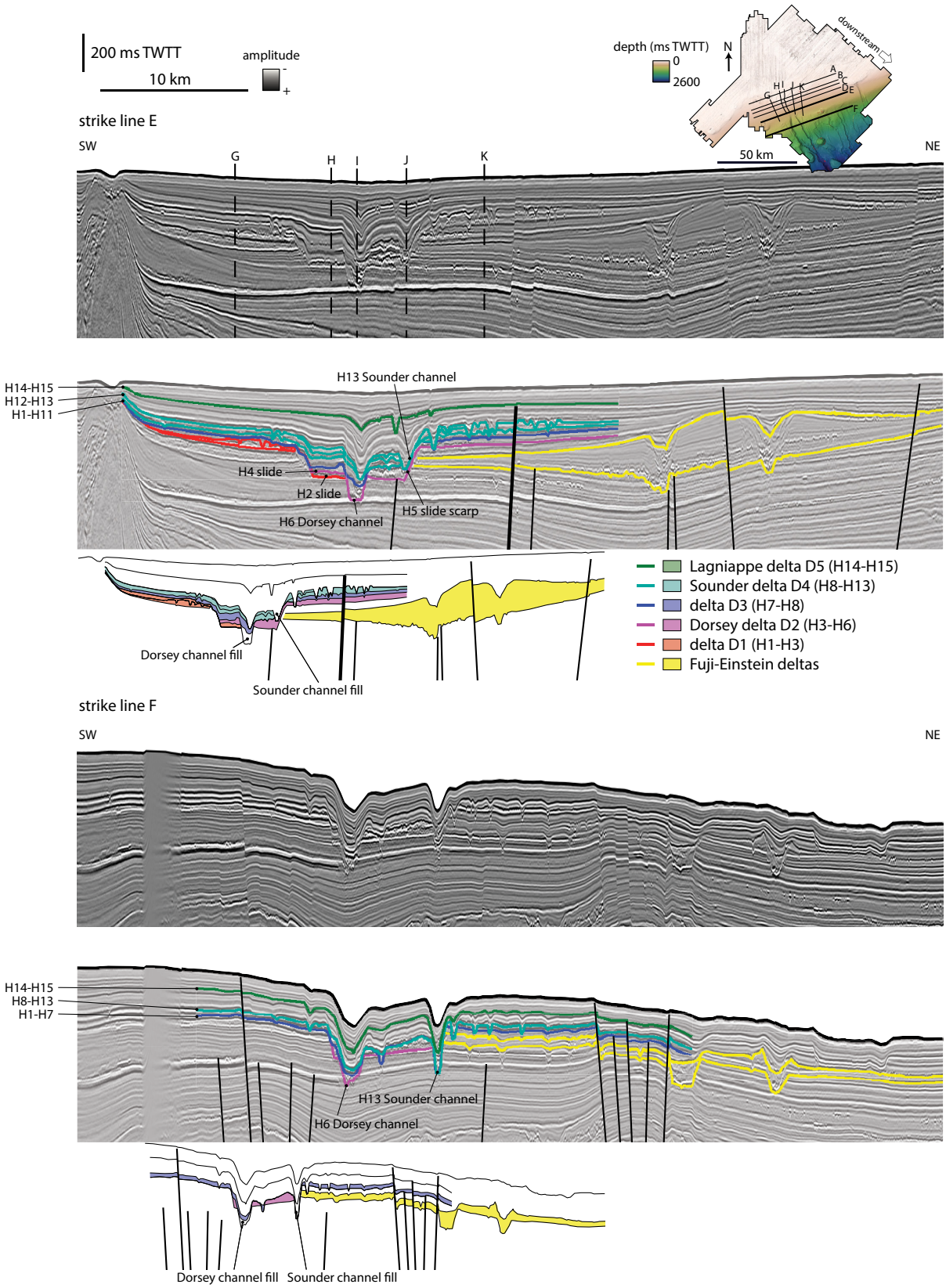

Figure 4 (*continued*).

another delta deposited during OIS 8 (Fig. 3; Kindinger, 1989; Kolla et al., 2000; Roberts et al., 2004). Consistent with delta seismic-facies models (e.g., Berg, 1982), the GOMSSRC core VK774c1 shows that the OIS 8 delta lobe becomes sandier up section (Figs. 3A and 4B; Roberts et al., 2004).

DATA AND METHODS

We used the prestack time-migrated Kirchhoff 3-D seismic-reflection volume B-32c-93-LA in the eastern Gulf of Mexico (Triezenberg et al., 2016; Kluesner et al., 2024) to document the interaction of delta sedimentation, mass wasting, and the formation of the Dorsey and Sounder submarine channels (Supplemental File S1[2]). Peak frequency ranges from ~30 Hz to 50 Hz in the shallow interval (Fig. 3A). Assuming seismic velocities of 1500–2000 m/s (Roberts et al., 2004), wavelengths are 50.0–66.7 m (12.5–16.7 m limit of separability; Brown, 2011). Kolla et al. (2003) used an average velocity of 1620 m/s to tie the GOMSSRC core VK774c1 to seismic-reflection data (Fig. 3). The 3-D seismic-reflection data were processed to zero phase with a lateral bin spacing of 25 × 25 m and a vertical sample rate of 4 ms TWTT.

We mapped 16 horizons (Supplemental File S2), based on continuity and terminations of seismic reflections in cross section (Mitchum et al., 1977) across an ~40 × 30 km area of the B-32c-93-LA survey (Figs. 4–6). The deepest horizon is just above OIS 13, which is represented by a condensed, muddy section in core VK774c1 (Fig. 3; Kolla et al., 2003; Fillon et al., 2004; Roberts et al., 2004). The shallowest horizon is the seafloor. We named these horizons in order, from base to top, H1 to H16; Figures 4 and 5 show strike and dip profiles, respectively, and Figure 6 shows maps of horizons (Supplemental Files S3 and S4). In general, because a delta thins from axis to margin (e.g., Fig. 2A), its multiple bounding and internal horizons appear to merge into a single reflection at its margin. This is why many horizons correspond to a single reflection at the margins of deltas in Figures 4 and 5. For example, in Figure 4B, the base and top horizons, H14 and H15, respectively, of Lagniappe delta D5 merge into a single reflection at the southwestern margin of the delta; this single reflection comprises the two overlapping base and top horizons, and it is labeled H14-H15 in the figure. Figure 7 shows maps of delta thicknesses, whereas Figure 8 shows cumulative thickness measured from base horizon H1 to progressively increasing horizons, i.e., between horizons H1 and H2, then H1 and H3, and so on until H1 and H16 (seafloor). For all horizons except the seafloor reflection, we found troughs to be the most consistent regionally mappable events (Figs. 3–5). We generated a semblance attribute volume, which compares similarity between adjacent seismic traces (Bahorich and Farmer, 1995), using a 12 sample vertical window. The semblance attribute was draped on horizon maps to highlight faults, landslides, and channels (Fig. 9). In semblance attribute maps, faults can correspond to low semblance values (high dissimilarity). We also interpreted faults based on reflection offset, and we accounted for them in horizon interpretations (Supplemental File S2). We used published horizons bounding the nearby Fuji-Einstein delta complex, active during OIS 20, and, possibly the preceding OIS 22 lowstand, for additional stratigraphic context of the margin (Figs. 4 and 5; Sylvester et al., 2012). Later, we discuss the evolution of the Dorsey-Sounder delta complex relative to the Fuji-Einstein delta complex. Ages were interpreted from GOMSSRC core VK774c1, which was recovered from the Lagniappe and predecessor deltas younger than OIS 14, based on ^{14}C and oxygen isotope stratigraphy (Fig. 3; Fillon et al., 2004).

[2]Supplemental Material. Supplemental File S1: Seismic-reflection data (SEG-Y). Zenodo repository (https://zenodo.org/records/15857064). Supplemental File S2: Horizons H1–H15 and seafloor (compressed [zipped] folder). Supplemental File S3: Animation of depositional-strike profiles from proximal to distal (MP4 file). Supplemental File S4: Animation of horizon maps arranged from base to top, H1–H15 (MP4 file). Please visit https://doi.org/10.1130/GEOS.S.30887087 to access the supplemental material; contact editing@geosociety.org with any questions.

RESULTS

Seismic Stratigraphy

On the mid- to outer shelf, horizons are even and parallel to each other and ~200 ms TWTT thick altogether (Fig. 4A; Supplemental File S3). Downstream, to the south, the interval thickens and shows at least five sets of clinoform reflections on the shelf (Fig. 5). Each clinoform set represents progradation of a delta (Berg, 1982). Just beyond the shelf edge, the delta interval thickens to almost 600 ms TWTT (Figs. 4C; Supplemental File S3). We correlated the age picks in GOMSSRC core VK774c1 with five deltas, D1 to D5, from old to young (Figs. 3–5; Kolla et al., 2003; Fillon et al., 2004; Roberts et al., 2004). The deltas were probably deposited one at a time during glacio-eustatic sea-level lowstands since OIS 13 (Fig. 3; Fillon et al., 2004):

(1) The basal delta, D1 (horizons H1–H3), was deposited after OIS 13, during the OIS 12 lowstand (Figs. 3 and 6, H1–H3). Horizon H1 is the base of the delta defined by downlapping clinoform foresets (Figs. 4B and 5G–5J). Horizon H2 truncates the delta at the shelf edge (Figs. 4B, 4C, and 5H). Horizon H3 is the delta top.
(2) The "Dorsey" delta D2 (horizons H3–H6) is named after the Dorsey submarine channel, which eroded the delta top at horizon H6 (Fig. 6, H3–H6). Horizon H3 is the base of the delta defined by downlapping foresets (Figs. 4B and 5I). Horizons H4 and H5 are within the Dorsey delta; they truncate clinoforms at the shelf edge (Figs. 5H, 5J, and 6, H4–H5). The margin of the delta was sampled in core VK7741c1, which indicates deposition during OIS 10 (Fig. 3).
(3) Roberts et al. (2004) characterized the next delta D3 (horizons H7 and H8), which was deposited during OIS 8 (Figs. 3 and 6, H7 and H8). Horizon H7 is the base of the delta; H8 is the top, as well as the base of the overlying delta D4, "Sounder" delta (Figs. 4B, 4C, and 5G).
(4) The "Sounder" delta D4 (horizons H8–H13) is named after the Sounder channel, which is incised into the delta top at horizon H13 (Fig. 6, H8–H13). Horizons H10–H12 are within the Sounder delta and truncate clinoforms at

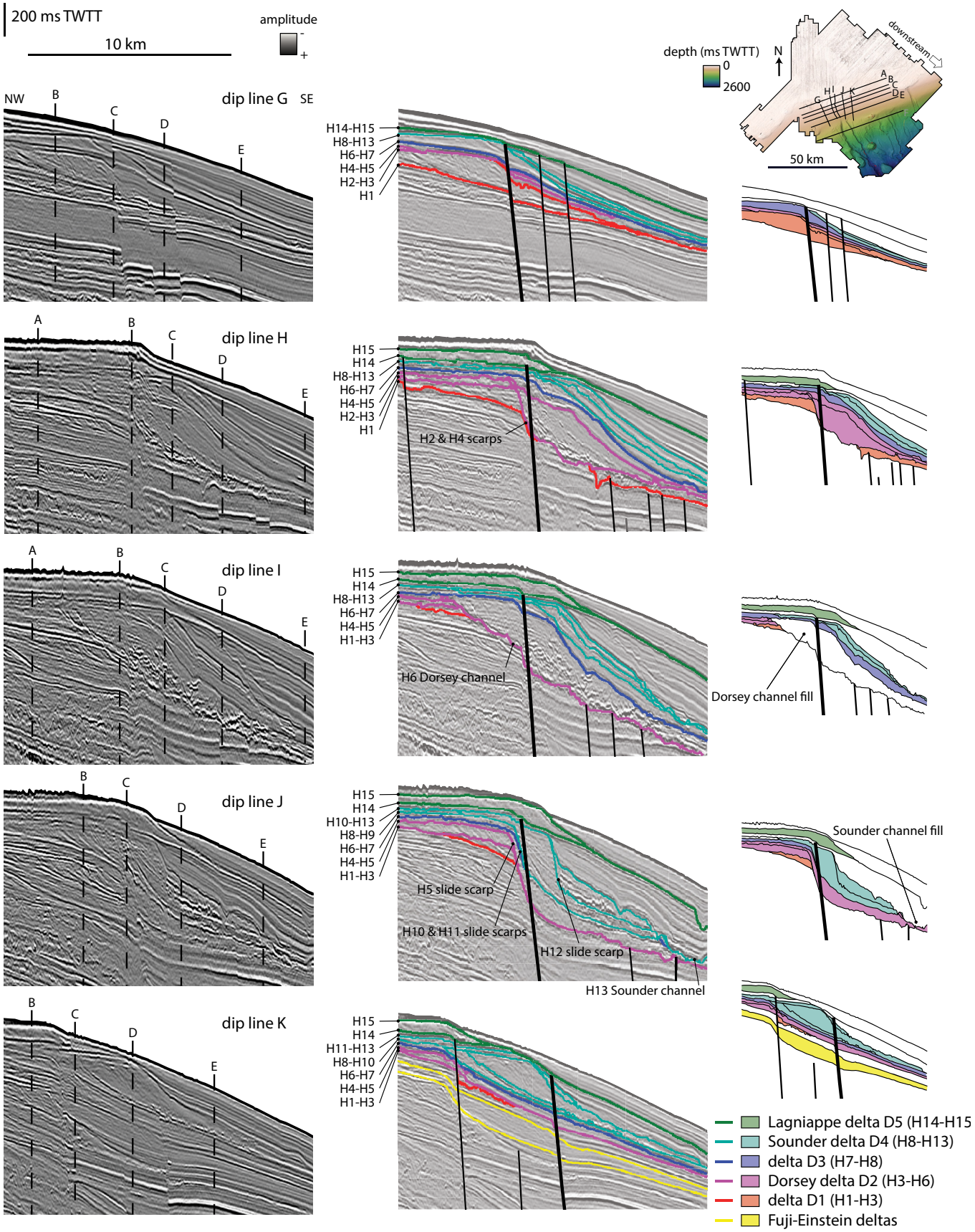

Figure 5. Depositional-dip profiles arranged from west to east: profiles G–K. Steeply dipping black lines of interpreted profiles are faults. Prominent shelf-edge growth fault is indicated by bold black lines. See Figure 6, H1 and H9, for map trace of this fault. See Figure 1 for profile locations. TWTT—two-way traveltime.

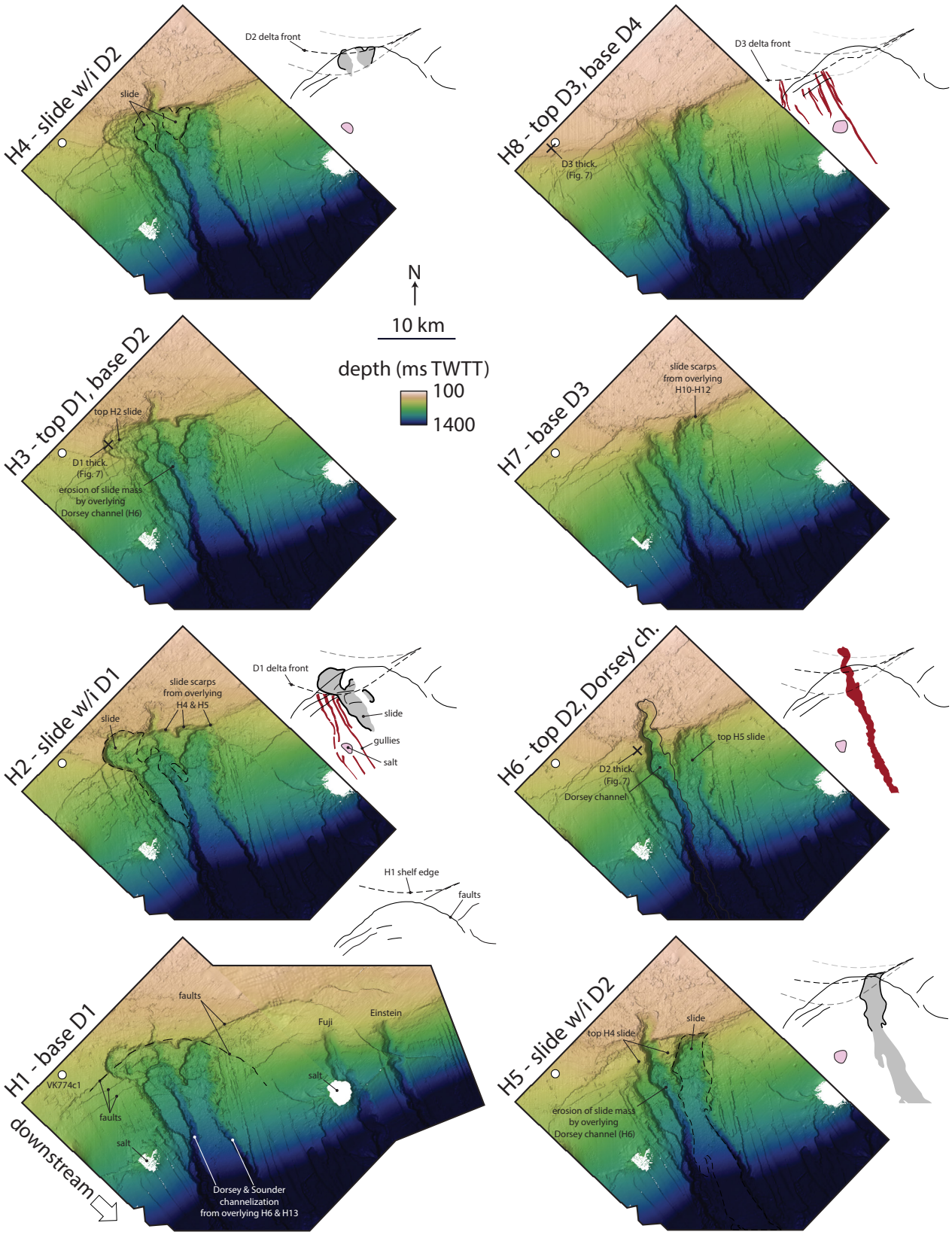

Figure 6. Horizon maps arranged from base to top: H1–H15. Faults, salt, and VK774c1 locations are indicated in map H1. Other maps show outlines of extents of submarine landslides and other features. The thickest points of deltas (see Fig. 7) are indicated on the top horizons of individual deltas. Line-drawing traces of initial horizon H1 and younger horizons with landslides (gray; scarps are emboldened black lines at their upstream margins) and channels (red), including gullies near delta tops, are to the right of some maps. Dashed lines are delta fronts. See also Supplemental File S4 (text footnote 2). TWTT—two-way traveltime. (*Continued on following page.*)

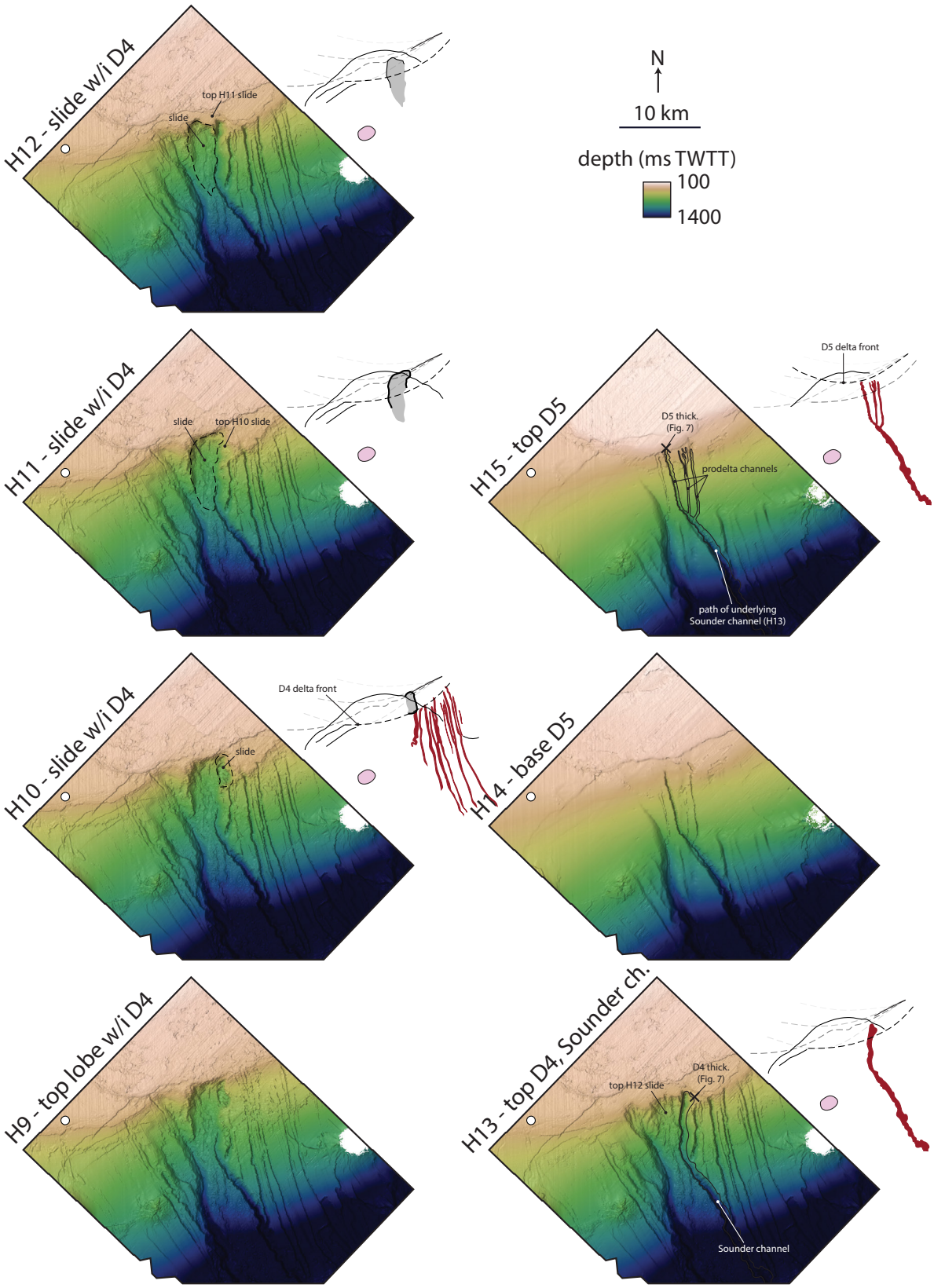

Figure 6 (*continued*).

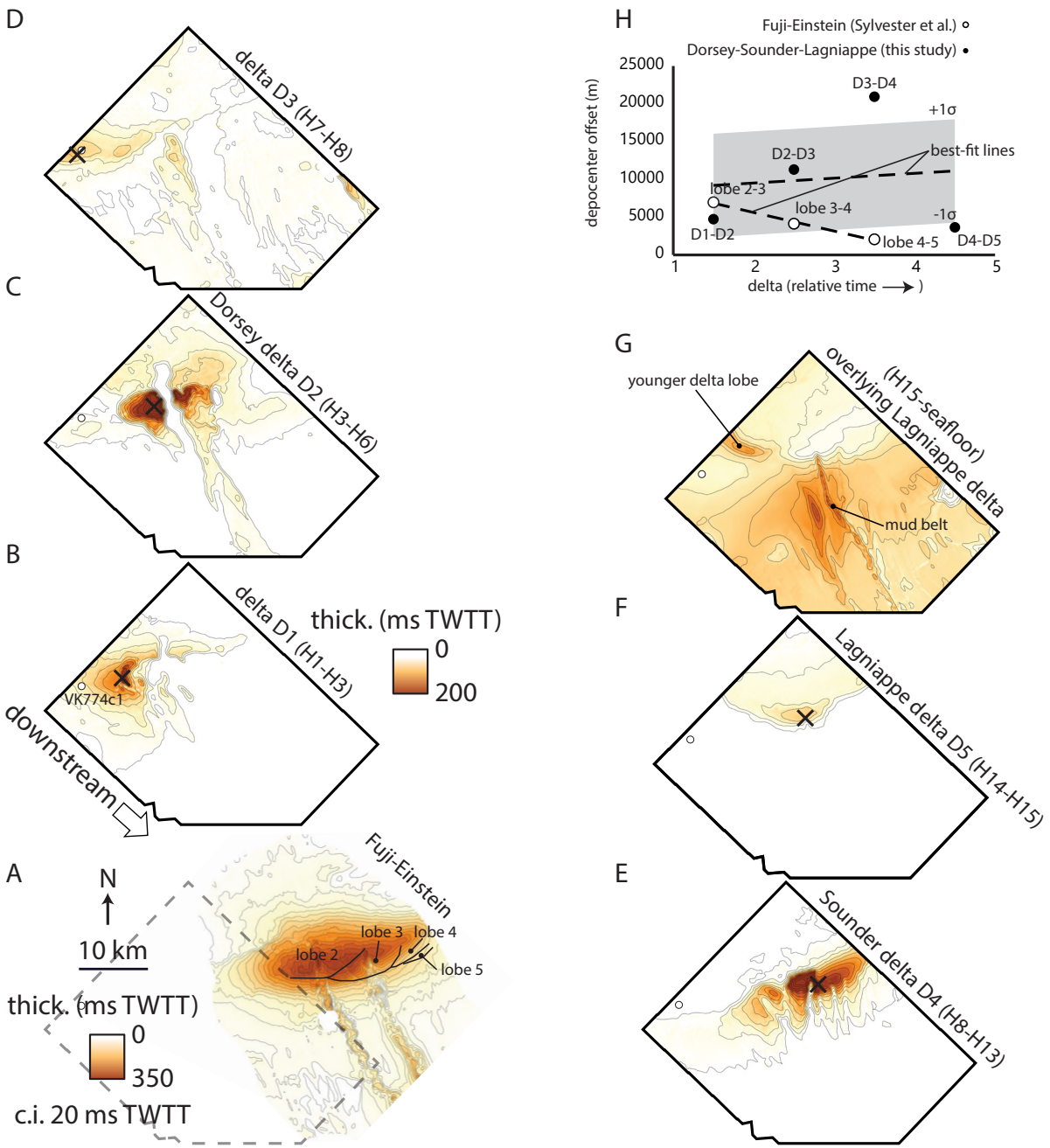

Figure 7. Thickness maps of deltas. (A) Fuji-Einstein delta complex. (B) Delta D1. (C) Dorsey delta D2. (D) Delta D3. (E) Sounder delta D4. (F) Lagniappe delta lobe D5. (G) Thickness from horizon H15 to seafloor, including a younger Lagniappe delta lobe and mud belt (cf. Sylvester et al., 2012). Details of this interval can be found in Kolla et al. (2000) and Roberts et al. (2004), and references therein. (H) Plot of distances between the thickest points of deltas (depocenter offset) for Sounder-Dorsey-Lagniappe deltas D1–D5 (this study) and the Fuji-Einstein delta complex (Sylvester et al., 2012). TWTT—two-way traveltime; c.i.—contour interval.

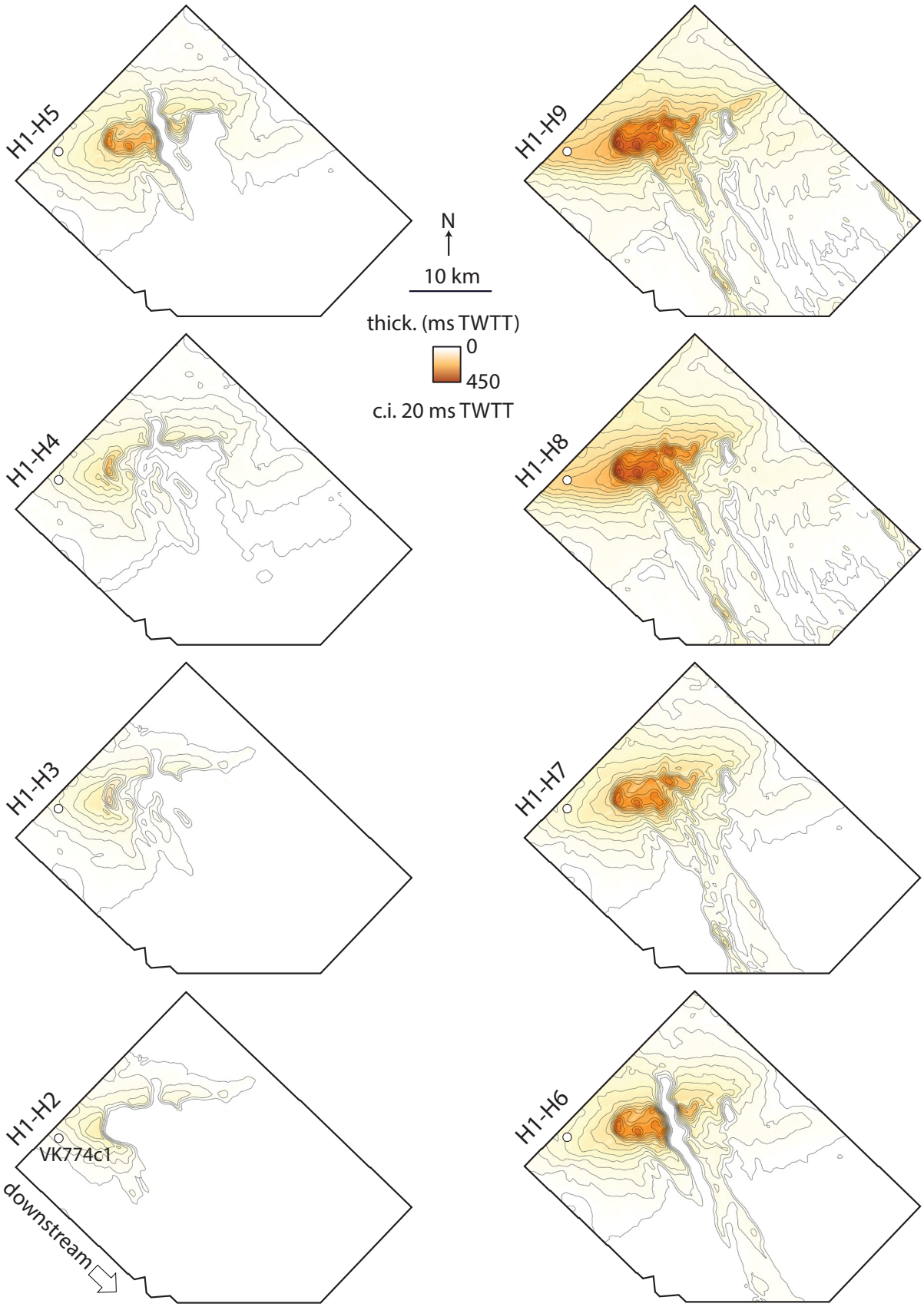

Figure 8. Cumulative thickness measured from base horizon H1 to progressively increasing horizons, i.e., between horizons H1 and H2, then H1 and H3, until H1 and H16 (seafloor). Also included is plot of standard deviation of thickness and mean thickness for each interval measured between H1 and H15. TWTT—two-way traveltime; c.i.—contour interval. (*Continued on following page.*)

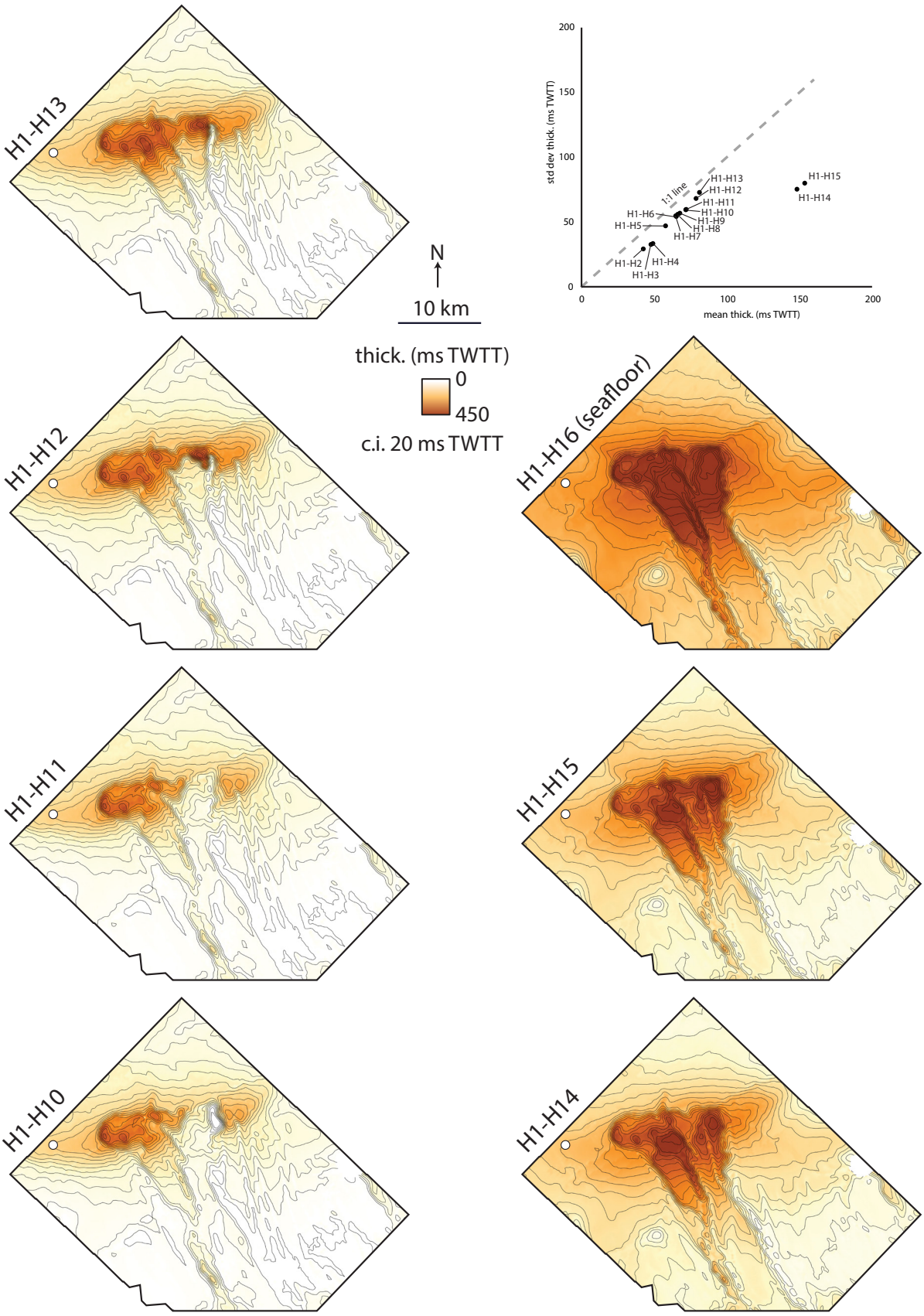

Figure 8 (*continued*).

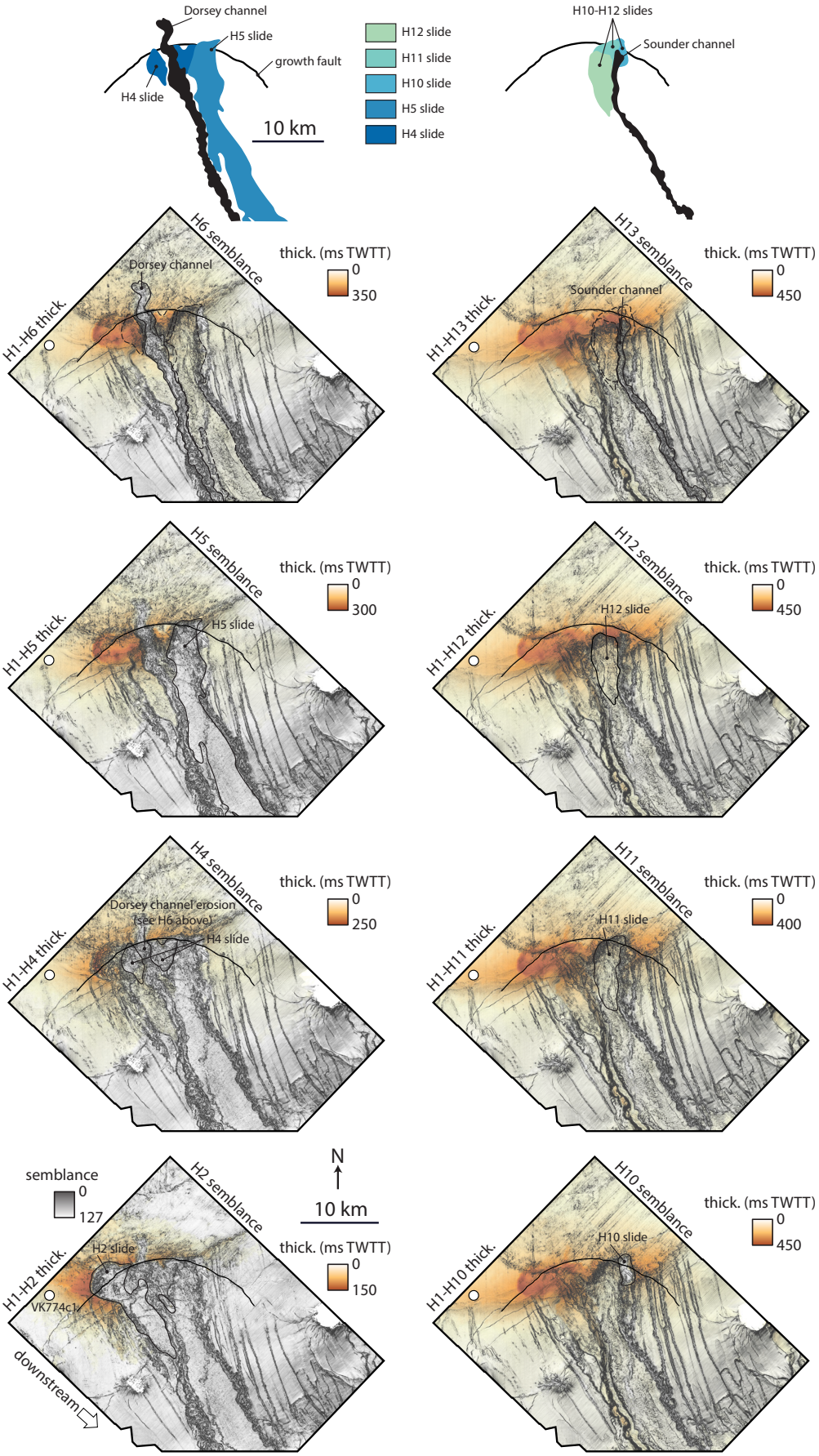

Figure 9. Submarine channels and landslides. Top: Line drawing traces of landslides and subsequent channels: Dorsey channel to left and Sounder channel to right. Landslide polygons are colored from early (dark blue) to late (light green). Channels are black polygons. Below: Co-rendered semblance attribute and thickness maps of channels and landslides. Left: Landslides forming at horizons H2, H4, and H5 and Dorsey channel forming at horizon H6. Right: H10–H12 landslides and Sounder channel forming at H13. Dashes lines at horizons H6 (Dorsey) and H13 (Sounder) are former locations of landslides influencing channelization of those deltas. TWTT—two-way traveltime.

the shelf edge (Figs. 4C, 4D, 5J, and 6, H10–H12). The thickest part of the Sounder delta is ~20 km to the east of core VK7741c1 (Fig. 7E). At the core hole, horizons H8–H13 have converged to a single reflection as a result of depositional thinning toward the delta margin (Figs. 3 and 4B). There, the Sounder delta overlies the OIS 8 delta D3, and it is well below an OIS 5 condensed section. In sequence, then, the Sounder delta was deposited during OIS 6, which is the next lowstand period in the interval of interest; however, the Sounder delta margin reflection does not align with OIS 6 in VK7741c1. Rather, the Sounder delta margin falls ~6 m below the OIS 7 condensed section, near the top of OIS 8 (Fig. 3A). That said, a 6 m offset is smaller than the limit of separability of the seismic-reflection data; a seismic-core mistie of that scale is not surprising. It seems most likely that the Sounder delta was deposited during the OIS 6 lowstand, after OIS 8, since it is compensationally stacked to the east atop OIS 8 delta D3 (Figs. 4 and 7E).

(5) A lobe, delta D5, of the Lagniappe delta complex (horizons H14–H15) is at the top of the interval of interest (Fig. 6, H14 and H15). Horizons 14 and 15 are the base and top, respectively, of a clinoform set that prograded to the south, across the shelf (Figs. 5H–5K). The delta lobe overlies the OIS 5 condensed section in core VK7741c1 (Fig. 3; Roberts et al., 2004); the Lagniappe delta complex is thought to have been active during OIS 4 and 2 lowstands (Kolla et al., 2000). Small channels are incised into the top of delta D5 at horizon H15; these channels coalesce downstream and follow the path of the underlying Sounder channel (Fig. 6, H15). More deposits of the Lagniappe delta complex overlie H15; they appear to prograde to the west of the area of interest, parallel to the shelf (Figs. 1C, 4, and 7G; Roberts et al., 2004).

Growth Faults and Submarine Landslides

At the shelf edge, deltas D1, D2 (Dorsey), and D4 (Sounder) are erosionally truncated and offset by growth faults, i.e., showing decreasing throw up section (e.g., Figs. 4 and 5), dipping to the south into the basin. It is unlikely that decreasing throw up section is a result of increasing seismic velocity with depth; for example, in Figure 5G, the reflection offset across the prominent shelf-edge growth fault (indicated by a bold black line) decreases by a factor of ~0.5 from ~600 m below the seafloor to ~200 m below the seafloor, but velocity only decreases by a factor of ~0.85 (i.e., from ~2000 m/s to ~1700 m/s) at those depths in the Gulf of Mexico (Cook and Sawyer, 2015). In addition, the fault offset decreases to near zero at the base of the Lagniappe delta, horizon H14 (bold black line in Fig. 5). We mapped erosional truncation at horizons H2 (truncates delta D1), H4 and H5 (Dorsey delta D2), and H10–H12 (Sounder delta D4; see Figs. 4–6). At the shelf edge, the truncation surfaces show scoop-shaped headscarps that occur along the trace of a broad growth fault at the shelf edge (Figs. 6 and 9); this fault is highlighted as a basinward-dipping, relatively bold black line in Figures 4 and 5, and it is identified in maps of Figure 6, H1 and H9. Downstream of the headscarps, the horizons are overlain by chaotic seismic facies with irregular, blocky texture in map view (Fig. 9). In contrast, the reflections between horizons H7 and H8 of delta D3 and between horizons H14 and H15 of the Lagniappe delta are intact clinoform sets, which thin toward the shelf edge (delta D3) or prograde over growth faults with little offset (Lagniappe delta D5; Figs. 4 and 5). We interpret the scoop-shaped truncation surfaces, horizons H2, H4, H5, and H10–H12, to be at least six submarine landslide scarps, which are overlain by mass-transport deposits in their downstream reaches (Fig. 9). In addition, we think the prominent shelf-edge growth fault promoted delta-front failure because of the spatial and temporal correspondence of the movement of the fault and the episodes of landsliding during delta D1–D4 deposition. We measured the runout distance of landslides based on their thicknesses measured between their bounding horizons, from their headscarps to the pinchout of the chaotic seismic facies (Fig. 9). The runout distance of these landslides is up to 33 km long, with the majority <10 km (Fig. 9). For context, Moscardelli and Wood (2016) reported the median length of a global selection of 247 submarine landslides to be ~15 km.

Delta Stacking

To quantify delta stacking since OIS 13, we measured the offset distance between the thickest points of successive deltas, i.e., the distance between delta D1 and D2, D2 and D3, and so on. The Dorsey-Sounder-Lagniappe deltas D1–D5 showed a wide range of offset, from ~1 km to 20 km, with considerable variability (standard deviation ~7 km). Offset distances increased from several to >20 km during deposition of deltas D1–D4, dominated by submarine landslides, which removed large portions of delta D1 and led to isochron thickening within landslide scarps of Dorsey delta D2 and Sounder delta D4 (Fig. 7). As the major landslides are distributed along the trace of a broad shelf-edge growth fault (Fig. 9), the offset of the thickest preserved intervals can be quite large from one delta to the next (e.g., from D3 to D4). The sediment-laden flows from these deltas were likely captured by the steep landslide scarps at the shelf edge, localizing deposition there. Later, the Lagniappe delta D5, lacking evidence of significant landsliding, was deposited in close proximity to its predecessor Sounder delta D4.

To further explore depositional patterns, we compared the standard deviation of thicknesses to the mean thickness measured from base horizon H1 to progressively increasing horizons, i.e., between horizons H1 and H2, then H1 and H3, and so on until H1 and H16 (seafloor; see Fig. 8). The trend of that relationship shows how thickness variability evolved during delta complex assembly (cf. coefficient of variation in deposition between two stratigraphic surfaces of Straub and Pyles, 2012). The interval dominated by landsliding, horizons H1–H13 of deltas D1–D4, shows a gradual increase in the standard deviation of thickness from nearly 70% of the mean to ~90% (Fig. 8). That is, as sediment accumulated, the distribution of thicknesses became increasingly more variable. This is because, although deposition can smooth some

topography by gradually filling lows, repeated landsliding resets the topography with rough surfaces. Eventually, after Sounder delta D4 (horizon H13), the standard deviation of thicknesses did not change much with increasing mean thickness as the deltas accumulated on the shelf margin. As a result, the standard deviation of thickness is ~50% of the mean for the H13–H15 interval. Without landslides, intact clinoform sets thin into the basin, where seismic reflections are more continuous, draping topography (Figs. 4 and 5).

Submarine Channels

The most prominent submarine channels of the interval of interest, Dorsey (horizon H6) and Sounder (horizon H13) incised into delta tops D2 and D4, respectively, originated from landslide scarps (Fig. 9). The fill of the Dorsey and Sounder channels appears to comprise a chaotic mix of low- and high-amplitude seismic reflections (Figs. 4B and 5I for Dorsey channel fill), which transition downstream to more organized stacks of channel-form high-amplitude reflections a few hundreds of meters wide (Figs. 4D–4F; Supplemental File S3). Landslides occurred near the thicker delta apices (Fig. 7), and their steep failure scarps captured prodelta sediment-gravity flows. Many flows probably followed this path of steepest descent into deep water and eventually carved meandering submarine channels. To illustrate the scarp morphology that promoted channel formation, Figures 5G–5I show three depositional-dip profiles of Dorsey delta D2: (1) the shelf edge to open slope southwest from the horizon H4 landslide (Fig. 5G); (2) the horizon H4 landslide scarp, which would approximate the seafloor postfailure and prior to Dorsey channel formation (Fig. 5H); and (3) the horizon H6 Dorsey channel thalweg (Fig. 5I). In Figure 5, Dorsey horizons H3–H6 of the shelf-edge to open-slope profile G are lower gradient and smooth, except for some minor fault offsets, compared to horizon H4 of the landslide scarp profile H and horizon H6 of the channel thalweg profile I. High-relief (hundreds of milliseconds TWTT) Dorsey delta D2 clinoforms downlap horizon H4 to heal the landslide scarp topography. The Dorsey channel thalweg horizon H6 truncates those clinoforms in profile I; this truncation is also shown in strike view in Figures 4B–4D. In addition, the Dorsey channel appears to have eroded ~4 km from the shelf edge, in an upstream direction (Fig. 9, H6 semblance map). Figure 10 illustrates a likely sequence of events once a delta prograded to the shelf edge: (1) A delta front failed at a shelf-edge fault, which created a steep landslide scarp; (2) the scarp

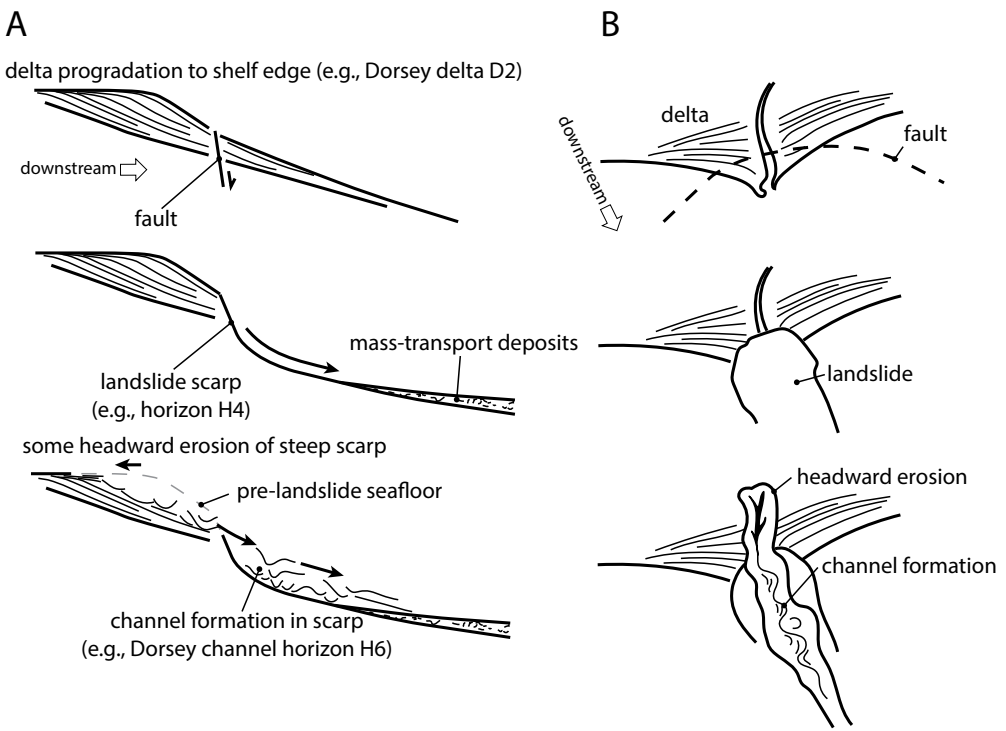

Figure 10. Conceptual diagram of submarine-channel formation based on Dorsey delta D2. (A) Cross-sectional evolution. (B) Map-view evolution. Top: Delta progrades to shelf-edge fault. Middle: Delta-front failure. Bottom: Channel formation in landslide scarp.

captured and redirected delta progradation; and (3) a local knickpoint eventually formed at the shelf-edge growth fault, where a submarine channel initiated and eroded headward. The Sounder channel (horizon H13) appears to have had a similar evolution, but without much headward erosion of the delta topset (Fig. 9, H13 semblance map). Downstream of landslide scarps, mass-transport deposits guided channel orientation—channels avoided topographic highs of the mass-transport deposits (Fig. 9).

Other channels beyond the shelf edge are much smaller, straighter gullies, which are distributed across delta fronts (Fig. 6). A few smaller tributary channels emanate from the Lagniappe delta D5; they coalesce downstream and reoccupy the underlying Sounder channel (Fig. 6, H15). While reoccupation has been interpreted for fluvial channels (e.g., Mohrig et al., 2000), it is less commonly documented, in 3-D, for submarine systems (although, an exception is presented in Jobe et al., 2015). Almost all the channels in the study area, from the large Dorsey and Sounder channels to the smaller gullies, formed stratigraphically near delta tops at the shelf edge (e.g., horizons H2 top delta D1, H6 top Dorsey delta D2, H8 top delta D3, H10 and H13, both near top Sounder delta D4, and H15 top Lagniappe delta D5).

DISCUSSION: STRATIGRAPHIC EVOLUTION OF DELTAS IN UNSTABLE SHELF MARGINS

It has been stated that deltas lack a "pure" delta-type shape and depositional pattern (Berg, 1982), with variation as a result of wave, tide, and fluvial influences (Galloway, 1975; Bourget et al., 2014; Ainsworth et al., 2011, 2019); however, clinoform seismic reflections are common characteristics of subsurface deltas. Indeed, Figure 2 shows an ideal wave-influenced river delta in the northeastern Gulf of Mexico, the Fuji-Einstein delta complex (Sylvester et al., 2012). There is a continuous transition from delta lobes to slope-channel and overbank deposits, producing well-developed, more-or-less intact shelf-margin clinoforms that are similar to generalized models (Fig. 2D; e.g., Berg, 1982). Recent surveys of modern deltas have provided more quantitative constraints on the influence of waves and tides on river-delta morphology (e.g., Nienhuis et al., 2015, 2020), and physical experiments and computational approaches have tested how changing sea level influences depositional patterns at scales ranging from 10^1 m^2 to 10^8 m^2 in area (e.g., Straub, 2019; Willis and Sun, 2019; Hariharan et al., 2022). However, there has been less effort made to understand the shape and depositional pattern of deltas in unstable shelf margins, although deltaic influences on shelf-edge instability have been explored for decades (e.g., Coleman et al., 1983). In the northeastern Gulf of Mexico, aside from obviously disrupting the shelf-margin clinoform stratigraphy typical of deltas (Figs. 4 and 5; Supplemental File S3), the Dorsey-Sounder landslides (1) modified delta compensational stacking, which is arguably the quintessential lobe-scale autogenic process; (2) led to atypical basin filling, reflected in the evolution of thickness variability; and (3) controlled submarine-channel formation and deep-water sediment delivery.

Delta Compensational Stacking

Compensational stacking is preferential deposition in topographic lows adjacent to previous deposits (Normark et al., 1993; Straub et al., 2009). If the Dorsey-Sounder deltas were compensationally stacked in an ordered way, we would expect similar, or progressively diminishing, offset distance from one delta to the next, as is the case for delta lobes 2–5 of the nearby Fuji-Einstein delta complex (Fig. 7H; see also fig. 6 of Sylvester et al., 2012). This is because the river delivering sediment to the Fuji-Einstein delta complex did not avulse a great distance from one delta to the next, but it appears to have systematically shifted toward the eastern topographic low away from previous deposits. Indeed, the depocenter offset diminished at a rate of ~2 km/delta shift from lobe 2 to 5 of the Fuji-Einstein delta complex.

In contrast, Dorsey-Sounder-Lagniappe delta offset distances progressively increased to >20 km (Fig. 8H). The deltas did not shift systematically from one to the next; they hopped all over the margin. This was likely a result of broadly and unpredictably distributed landslide scarps capturing flows and steering the deltas at the shelf edge. So, although depocenters D1–D5 shifted from one delta to the next, by our measure, they did not compensationally stack in an ordered way like those documented in the nearby Fuji-Einstein delta complex, which lacks large submarine landslides. Accordingly, Dorsey-Sounder deltas D1, D2, and D4, with landslides, show truncated clinoforms (Fig. 5) and thickness patterns different from the expected continuous thinning of depocenters toward delta margins (Fig. 11). This difference can be applied to predictions of the subsurface heterogeneity applicable to resource exploration and extraction, as well as evaluations of carbon storage potential, in similar settings. Whereas deltaic heterogeneity is commonly related to sea-level changes and varying wave, tide, and fluvial influences (Ainsworth et al., 2011; Willis and Sun, 2019), we show that the underlying fault and landslide framework also governs the thickness distribution and architecture of individual deltas.

Basin-Fill Thickness Variability

Attempts to measure variability of basin filling in smaller-scale physical experiments, in which sedimentation, subsidence, and stratigraphy can all be measured at relatively high spatial and temporal resolution, show a decreasing trend of standard deviation of sedimentation divided by subsidence between progressively increasing horizons (e.g., Sheets et al., 2002; Straub et al., 2009). The measure of this decreasing trend has been called the "compensation index." It is a result of local deposition and negligible subsidence during shorter time scales of observation, but more broadly distributed deposition across an entire subsiding basin during longer time scales (Straub et al., 2009). Although we interpreted the relative timing of deposition of field-scale deltas in the northeastern Gulf of Mexico (Fig. 3), age control is more poorly constrained; we are only confident in the insight that deltas prograded to the shelf edge, one at a time, during glacio-eustatic lowstands over the last 0.5 m.y. (Fillon

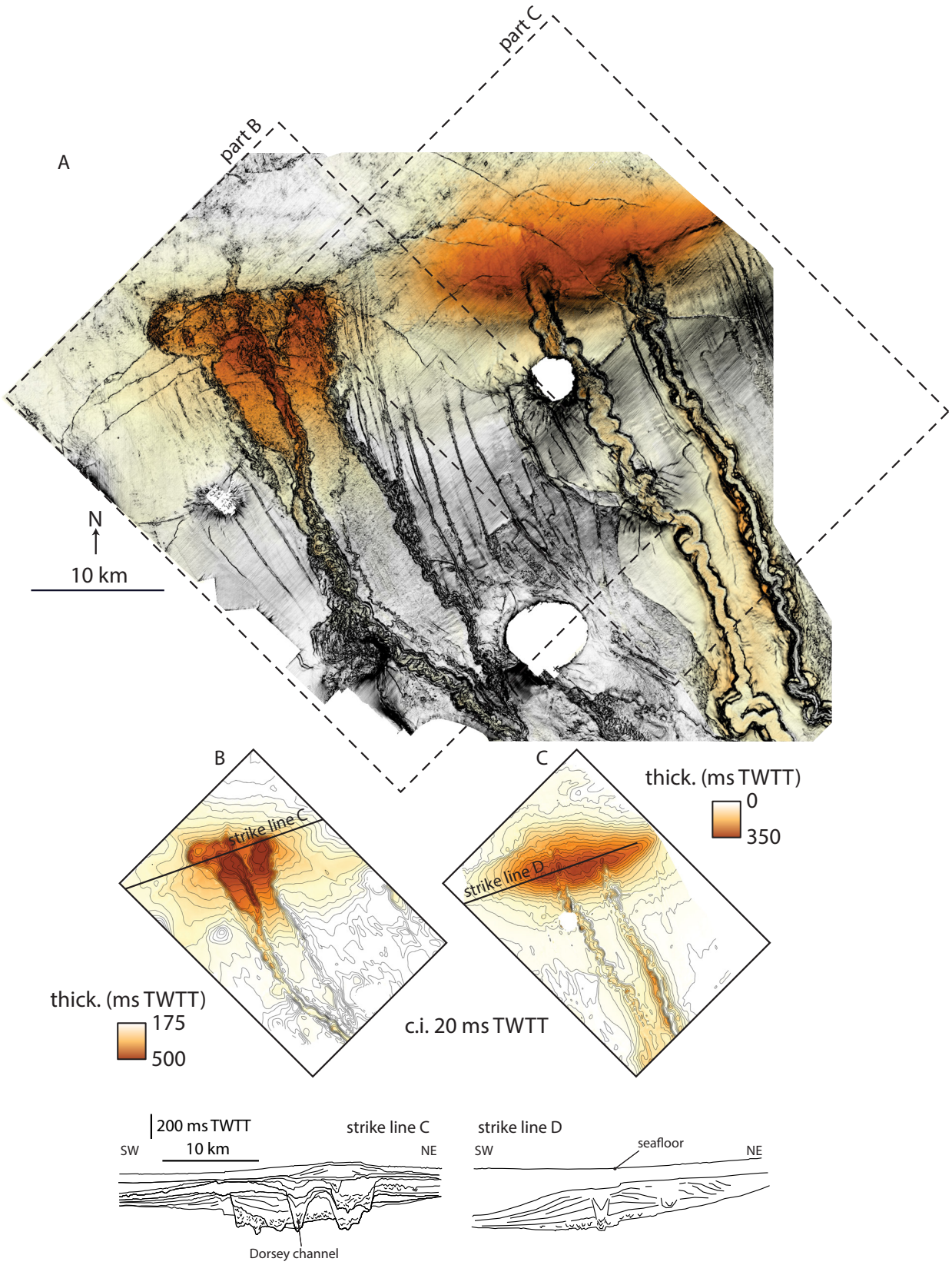

Figure 11. Landslide-influenced delta morphology comparison to "typical" Fuji-Einstein delta complex. (A) Co-rendered semblance attribute and thickness maps of the Dorsey-Sounder-Lagniappe delta complex (this study) and the Fuji-Einstein delta complex (Sylvester et al., 2012). Semblance attribute was extracted from horizon H1 (top Fuji-Einstein delta complex and base Dorsey-Sounder-Lagniappe delta complex). (B) Dorsey-Sounder-Lagniappe thickness. (C) Fuji-Einstein thickness. Below: line-drawing traces of Dorsey-Sounder-Lagniappe (left) and Fuji-Einstein (right) stratigraphy (from Fig. 4 strike lines C and D). TWTT—two-way traveltime; c.i.—contour interval.

et al., 2004). So, we could not measure sedimentation and subsidence rates like in a physical experiment. To characterize thickness variability, we simply plotted the standard deviation of thickness against the mean (Figs. 8 and 11C). Dorsey-Sounder delta-front landslides promoted increasing thickness variability measured over progressively longer time intervals during H1–H13 deposition. Increasing standard deviation with an increasing mean is not necessarily surprising. However, the standard deviation can be normalized as a proportion of the mean to yield the coefficient of variation. This coefficient of variation increased or stayed roughly the same during H1–H13 deposition (Fig. 12E), which is surprising. We discuss this result in the following paragraph, in the context of previous experimental work. For H1–H14 and H1–H15 thicknesses, after the landslides, the sedimentation pattern changed during deposition of the D5 lobe of the Lagniappe delta complex. As a result, the standard deviation of thickness stabilized with increasing mean thickness, and the coefficient of variation dropped. We can use the coefficient of variation to compare our field-scale results to other examples, including much smaller-scale physical experiments that are arguably applicable to a range of settings (cf. Straub and Pyles, 2012).

The eXperimental EarthScape XES-02 experiment was performed at St. Anthony Falls Laboratory, University of Minnesota, to investigate shelf-margin stratigraphic evolution in response to changing sea level (Strong and Paola, 2008; Martin et al., 2009). We used these experimental data, including a model comprising 1860 stratigraphic surfaces compiled by Sylvester et al. (2024), to measure thickness variability for comparison to our field example (Fig. 12B). Some of these surfaces are proportional slices between elevations defined by experimental scans. Notably, XES-02 had cohesionless sediment and lacked the landslides and submarine channels of the northeastern Gulf of Mexico margin. Fluvial erosion dominated the proximal part of the experimental basin, with relatively continuous shelf-margin clinoforms leading to a well-defined depocenter ~3.5 m downstream (Fig. 12B). XES-02 results resemble subsurface delta stratigraphy, especially in depositional-dip views (Fig. 12B). We plotted the standard deviation of thickness relative to mean thickness measured between the base of the model and progressively increasing surfaces, every 10th percentile surface (Figs. 12D and 12E). At first glance, the XES-02 trend of standard deviation of thickness with increasing mean thickness is similar to that of the Dorsey-Sounder deltas (Figs. 11C and 11D). However, the coefficient of variation tells a different story: Contrary to Dorsey-Sounder deltas, experiment XES-02 showed a nonlinear decrease in the coefficient of variation (Fig. 12E). Opposing trends are evident in Figure 12E, with initially increasing variability for the Dorsey-Sounder delta front with recurrent landslides, and a decay in variability according to a power law for XES-02 (cf. Sheets et al., 2002; Straub et al., 2009; Straub and Pyles, 2012). The sedimentation pattern changed in the Gulf of Mexico during deposition of the D5 lobe of the Lagniappe delta complex, characterized by intact clinoforms thinning into the basin and more continuous, draping reflection geometries. Consequently, the coefficient of variation decreased and settled at a standard deviation of ~50% of the mean, which is similar to XES-02. In this way, the statistics of basin filling can evolve differently depending on the abundance of roughness elements, like growth faults, submarine landslides, and channels, common to unstable margins.

Submarine Channel Formation and Deep-Water Sediment Delivery

In the nearby Fuji-Einstein part of the northeastern Gulf of Mexico margin, landslides did not significantly influence shelf-margin progradation or channelization, and there is a more continuous transition from delta clinoforms to slope-channel fill (Sylvester et al., 2012). Moreover, Fuji-Einstein submarine-channel initiation has been related to capture of prodelta sediment-gravity flows by gullies, a process that has also been interpreted in the Brunei Darussalam delta-fed margin (Straub and Mohrig, 2009; Straub et al., 2012). The Fuji-Einstein part of the margin lacks a significant basinward-dipping growth fault at the shelf edge and upper slope, although a Fuji delta lobe is offset by a growth fault on the shelf (Fig. 6, H1). Rather, at the shelf edge and upper slope, the Fuji-Einstein margin is defined by counterregional growth faults that localized deposition on their landward hanging walls (Sylvester et al., 2012). This is in contrast to the Dorsey-Sounder part of the margin, where landslides formed across basinward-dipping growth faults, and those landslides controlled the positions of channel heads and localized their downstream pathways. So, the importance of landslides in submarine-channel formation varies across the northeastern Gulf of Mexico, and through time, as the Lagniappe delta complex lacks the larger channels of the underlying Dorsey-Sounder deltas.

The Fuji-Einstein and Dorsey-Sounder depositional systems represent contrasting styles of delta-fed margin evolution: Fuji-Einstein is characterized by a continuous transition from deltas to slope-channel fill, producing well-developed shelf-margin clinoforms (Fig. 2), whereas the Dorsey-Sounder system is characterized by delta progradation to steep landslide scarps at the shelf edge (Fig. 11). These contrasting styles of margin evolution have been explored in numerical simulations of basin fill (e.g., Ross et al., 1994) and in more recent physical experiments (Abeyta et al., 2018). Abeyta et al. (2018) documented experimental cases in which terrigenous sediment delivery to deep water was influenced by shelf-margin clinoform geometry. A key control on whether shelf-margin clinoform progradation was maintained or sediment was bypassed into deep water was the balance between the slopes of the delta foreset and the underlying shelf margin. When the slope of the delta foreset was less than the slope of the underlying shelf margin, sediment was bypassed beyond the toe of slope into the deep basin. In the experiment, Abeyta et al. (2018) kept the slope of the underlying shelf margin constant but reduced the slope of the delta foreset by increasing the sediment concentration of sediment-gravity flows entering the basin (Kostic et al., 2002). Another way to promote sediment bypass in the experiment would be to simply have a delta prograde to an oversteepened position at the shelf edge; this is analogous to the landslide scarps of the Dorsey-Sounder shelf edge, where submarine-channel heads formed. In contrast, the Fuji-Einstein system is similar to the experimental case in which the delta foreset slope was approximately as steep

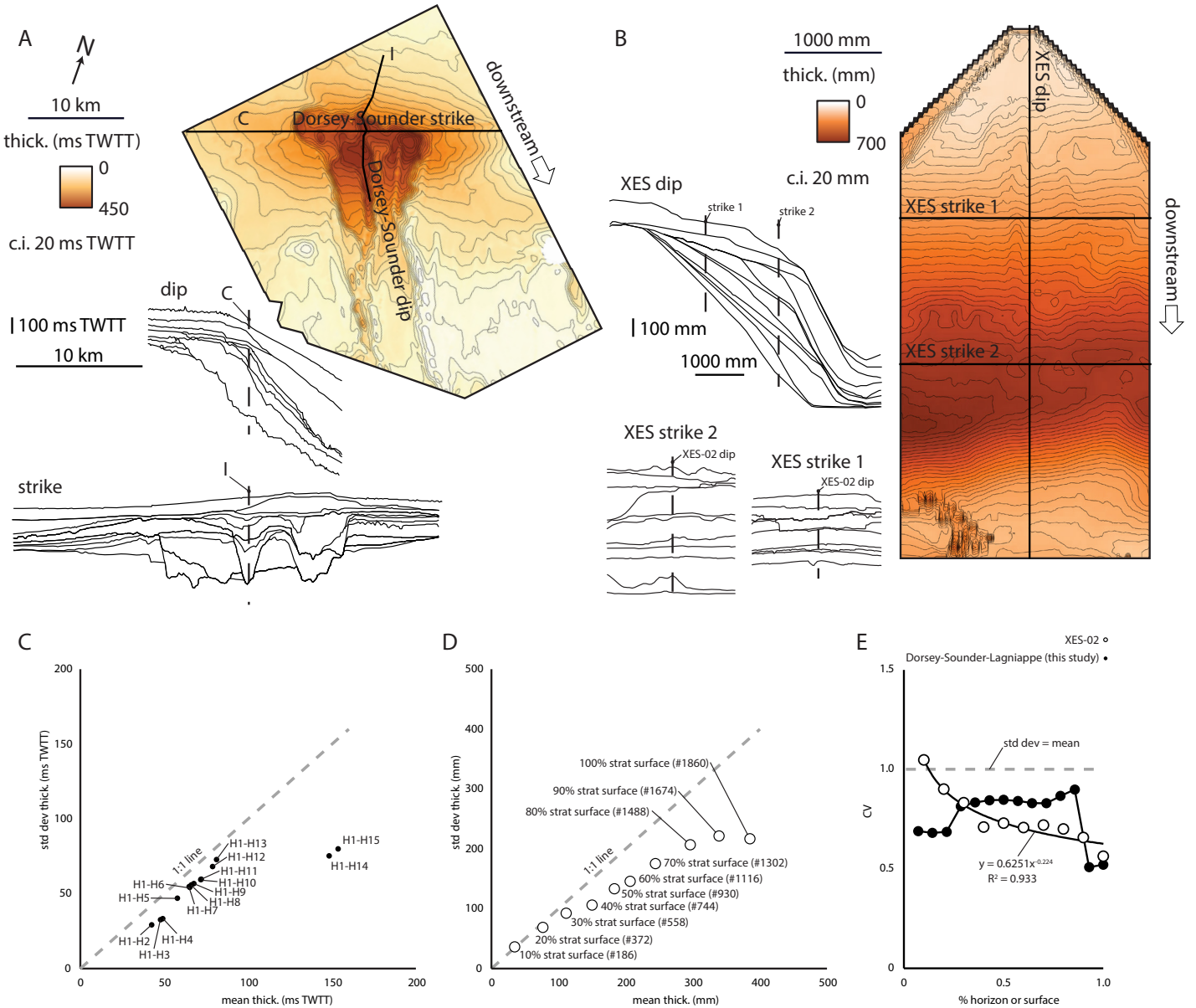

Figure 12. Landslide-influenced delta deposition comparison to experimental shelf margin. (A) Dorsey-Sounder-Lagniappe delta complex thickness (horizons H1–H15) and stratigraphy (depositional-strike profile C from Fig. 4; depositional-dip profile I from Fig. 5). (B) XES-02 experimental shelf-margin thickness and stratigraphy from Sylvester et al. (2024). (C) Plot of standard deviation of thickness and mean thickness measured between progressively increasing horizons of Dorsey-Sounder delta complex from Figure 8. Compare to part D. (D) Plot of standard deviation of thickness and mean thickness measured between the base of XES-02 model and progressively increasing surfaces, every 10th percentile surface. (E) Plot of coefficient of variation (CV) of thickness for Dorsey-Sounder-Lagniappe delta complex compared to XES-02 experiment. TWTT—two-way traveltime; c.i.—contour interval.

as or slightly steeper than the underlying shelf-margin topography (Abeyta et al., 2018). In that case, shelf-margin clinoform progradation was maintained throughout the experiment.

An implication of the Abeyta et al. (2018) experiment is that deep-water deposits composed of landslides and sandy submarine channel and fan systems might be a result of an oversteepened margin compared to the delta foreset, rather than sea-level change (e.g., Posamentier and Kolla, 2003). Sea-level changes might control delta migration across the shelf; indeed, shelf-edge delta deposition in the eastern Gulf of Mexico has been documented to occur during glacio-eustatic lowstands (Fillon et al., 2004). However, once a delta reaches the shelf edge, events that oversteepen the margin, such as landsliding, might promote a period of slope readjustment when terrigenous sediment is bypassed to deep water (Ross et al., 1994). This idea has obvious exploration significance in unstable margins: Recognition of delta-front landslides in seismic-reflection data or the presence of anomalous bathyal wedges stratigraphically sandwiched between shelf deposits in wells indicates an interval of sediment bypass to deep water (A. Pulham and T. Elliott, 2014, personal commun.).

CONCLUSION

In the northeastern Gulf of Mexico, five deltas were deposited one at a time during glacio-eustatic sea-level lowstands since OIS 14. Delta-front landslides formed along a prominent shelf-edge growth fault. These landslides truncated the clinoform stratigraphy typical of unperturbed deltas and localized deposition and submarine-channel formation. More specifically, deltas did not compensationally stack in an ordered way; instead, their offset distances progressively increased to >20 km as they preferentially filled broadly distributed landslide scarps. In addition, thickness variability increased over time as repeated landsliding reset the shelf-margin topography with rough surfaces. Landslide scarps also captured prodelta sediment-gravity flows, which carved meandering submarine channels. Downstream of landslide scarps, channels avoided the topographic highs of mass-transport deposits. Overlying the landslide-dominated Dorsey-Sounder interval, the Lagniappe system is characterized by more typical delta stratigraphy. The stratigraphic patterns and processes of deep-water sediment delivery are potentially different in unstable shelf margins compared to settings where intact clinoform sets initially thicken and then thin in the basin, producing the lenticular cross-sectional and overall map-view geometries typical of unperturbed delta stratigraphy.

ACKNOWLEDGMENTS

We are grateful to the U.S. Geological Survey (USGS) and the Bureau of Ocean Energy Management (BOEM) for sharing and hosting the seismic-reflection data used in this study at the National Archive of Marine Seismic Surveys (NAMSS). This work was supported by the sponsors of the University of Texas at Austin Quantitative Clastics Laboratory (https://qcl.beg.utexas.edu/). We thank AspenTech Epos™ Applications for subsurface interpretation. We thank David Mohrig and Hugh Daigle for insightful discussions about shelf-edge deltas and landslides. We thank reviewers Rebecca Englert and Vittorio Maselli for recommendations that improved the clarity of the manuscript and its figures and Science Editor David Fastovsky and Associate Editor Andrea Fildani for handling and evaluating our manuscript.

REFERENCES CITED

Abeyta, A., Foreman, B.Z., Swenson, J.B., Paola, C., and Mohr, J., 2018, Sink-to-source: Influence of offshore dynamics on upstream processes: Basin Research, v. 30, p. 783–798, https://doi.org/10.1111/bre.12280.

Ainsworth, R.B., Vakarelov, B.K., and Nanson, R.A., 2011, Dynamic spatial and temporal prediction of changes in depositional processes on clastic shorelines—Toward improved subsurface uncertainty reduction and management: American Association of Petroleum Geologists Bulletin, v. 95, no. 2, p. 267–297, https://doi.org/10.1306/06301010036.

Ainsworth, R.B., Vakarelov, B.K., Eide, C.H., Howell, J.A., and Bourget, J., 2019, Linking the high-resolution architecture of modern and ancient wave-dominated deltas: Processes, products, and forcing factors: Journal of Sedimentary Research, v. 89, p. 168–185, https://doi.org/10.2110/jsr.2019.7.

Allen, P.A., 2017, Sediment Routing Systems: The Fate of Sediment from Source to Sink: Cambridge, UK, Cambridge University Press, 422 p., https://doi.org/10.1017/9781316135754.

Anderson, J.B., and Fillon, R., 2004, Late Quaternary Stratigraphic Evolution of the Northern Gulf of Mexico Margin: Society for Sedimentary Geology (SEPM) Special Publication 79, 311 p., https://doi.org/10.2110/pec.04.79.

Anderson, J.B., Rodriguez, A., Abdulah, K.C., Fillon, R.H., Banfield, L.A., McKeown, H.A., and Wellner, J.S., 2004, Late Quaternary stratigraphic evolution of the northern Gulf of Mexico margin: A synthesis, *in* Anderson, J.B., and Fillon, R., eds., Late Quaternary Stratigraphic Evolution of the Northern Gulf of Mexico Margin: Society for Sedimentary Geology (SEPM) Special Publication 79, p. 1–23, https://doi.org/10.2110/pec.04.79.

Bahorich, M., and Farmer, S., 1995, 3-D seismic discontinuity for faults and stratigraphic features: The coherence cube: The Leading Edge, v. 14, p. 1053–1058, https://doi.org/10.1190/1.1437077.

Berg, O.R., 1982, Seismic detection and evaluation of delta and turbidite sequences: Their application to exploration for the subtle trap: American Association of Petroleum Geologists Bulletin, v. 66, p. 1271–1288, https://doi.org/10.1306/03B5A78C-16D1-11D7-8645000102C1865D.

Bourget, J., Ainsworth, R.B., and Thompson, S., 2014, Seismic stratigraphy and geomorphology of a tide or wave dominated shelf-edge delta (NW Australia): Process-based classification from 3D seismic attributes and implications for the prediction of deep-water sands: Marine and Petroleum Geology, v. 57, p. 359–384, https://doi.org/10.1016/j.marpetgeo.2014.05.021.

Brown, A.R., 2011, Interpretation of Three-Dimensional Seismic Data: American Association of Petroleum Geologists 42, 341 p., https://doi.org/10.1306/M4271346.

Campbell, K.J., 1999, Deepwater geohazards: How significant are they?: The Leading Edge, v. 18, no. 4, p. 514–519, https://doi.org/10.1190/1.1438329.

Carter, R.C., Gani, M.R., Roesler, T., and Sarwar, A.K., 2016, Submarine channel evolution linked to rising salt domes, Gulf of Mexico, USA: Sedimentary Geology, v. 342, p. 237–253, https://doi.org/10.1016/j.sedgeo.2016.06.021.

Clemenceau, G.R., and Miller, P.L., 1993, Fan-lobe geometry and reservoir sand characteristics of Ram/Powell Field, Deepwater Gulf of Mexico, *in* Technical Program for the 68th Annual Technical Conference and Exhibition of the Society of Petroleum Engineers: Houston, Texas, Society of Petroleum Engineers, paper SPE26441, p. 261–262, https://doi.org/10.2118/26441-MS.

Coleman, J.M., Prior, D.B., and Lindsay, J.F., 1983, Deltaic influences on shelfedge instability processes, *in* Stanley, D.J., and Moore, G.T., eds., The Shelfbreak: Critical Interface on Continental Margins: Society for Sedimentary Geology (SEPM) Special Publication 33, p. 121–137, https://doi.org/10.2110/pec.83.06.0121.

Cook, A.E., and Sawyer, D.E., 2015, The mud-sand crossover on marine seismic data: Geophysics, v. 80, no. 6, p. A109–A114, https://doi.org/10.1190/geo2015-0291.1.

Damuth, J.E., 1994, Neogene gravity tectonics and depositional processes on the deep Niger Delta continental margin: Marine and Petroleum Geology, v. 11, p. 320–346, https://doi.org/10.1016/0264-8172(94)90053-1.

Falivene, O., Frascati, A., Bolla Pittaluga, M., and Martin, J., 2019, Three-dimensional reduced-complexity simulation of fluvio-deltaic clastic stratigraphy: Journal of Sedimentary Research, v. 89, p. 46–65, https://doi.org/10.2110/jsr.2018.73.

Farre, J.A., McGregor, B.A., Ryan, W.B., and Robb, J.M., 1983, Breaching the shelfbreak: Passage from youthful to mature phase in submarine canyon evolution, *in* Stanley, D.J., and Moore, G.T., eds., The Shelfbreak: Critical Interface on Continental Margins: Society for Sedimentary Geology (SEPM) Special Publication 33, p. 25–39, https://doi.org/10.2110/pec.83.06.0025.

Fillon, R.H., Kohl, B., and Roberts, H.H., 2004, Late Quaternary deposition and paleobathymetry at the shelf-slope transition, ancestral Mobile River delta complex, northeastern Gulf of Mexico, *in* Anderson, J.B., and Fillon, R.H., eds., Late Quaternary Stratigraphic Evolution of the Northern Gulf of Mexico Margin: Society for Sedimentary Geology (SEPM) Special Publication 79, p. 111–141, https://doi.org/10.2110/pec.04.79.0111.

Galloway, W.E., 1975, Process framework for describing the morphologic and stratigraphic evolution of deltaic depositional systems, *in* Broussard, M.L., ed., Deltas: Models for Exploration: Houston, Texas, USA, Houston Geological Society, p. 87–98.

Godo, T.J., 2006, Identification of stratigraphic traps with subtle seismic amplitude effects in Miocene channel/levee sand systems, NE Gulf of Mexico, *in* Allen, M.R., Goffey, G.P., Morgan, R.K., and Walker, I.M., eds., The Deliberate Search for the Stratigraphic Trap: Geological Society, London, Special Publication 254, p. 127–151, https://doi.org/10.1144/GSL.SP.2006.254.01.07.

Hackbarth, C.J., and Shew, R.D., 1994, Morphology and stratigraphy of a mid-Pleistocene turbidite leveed channel from seismic, core and log data, northeastern Gulf of Mexico, *in* Bouma, A.H., and Perkins, B.G., eds., Submarine Fans and Turbidite Systems: Proceedings of the 15th Annual Research Conference: Houston, Texas, USA, Gulf Coast Section, Society for Sedimentary Geology (SEPM), p. 127–133.

Hage, S., Romans, B.W., Peploe, T.G.E., Poyatos-Moré, M., Ardakani, O.H., Bell, D., Englert, R.G., Kaempfe-Droguett, S.A., Nesbit, P.R., Sherstan, G., Synnott, D.P., and Hubbard, S.M., 2022, High rates of organic carbon burial in submarine deltas maintained on geological timescales: Nature Geoscience, v. 15, p. 919–924, https://doi.org/10.1038/s41561-022-01048-4.

Hampton, M.A., Lee, H.J., and Locat, J., 1996, Submarine landslides: Reviews of Geophysics, v. 34, p. 33–59, https://doi.org/10.1029/95RG03287.

Haq, B., and Milliman, J., 2023, Perilous future for river deltas: GSA Today, v. 33, no. 10, p. 4–12, https://doi.org/10.1130/GSATG566A.1.

Hariharan, J., Passalacqua, P., Xu, Z., Michael, H.A., Steel, E., Chadwick, A., Paola, C., and Moodie, A.J., 2022, Modeling the dynamic response of river deltas to sea-level rise acceleration: Journal of Geophysical Research: Earth Surface, v. 127, no. 9, https://doi.org/10.1029/2022JF006762.

Jobe, Z.R., Sylvester, Z., Parker, A.O., Howes, N., Slowey, N., and Pirmez, C., 2015, Rapid adjustment of submarine channel architecture to changes in sediment supply: Journal of Sedimentary Research, v. 85, p. 729–753, https://doi.org/10.2110/jsr.2015.30.

Kendrick, J.W., 2000, Turbidite reservoir architecture in the northern Gulf of Mexico deepwater: Insights from the development of Auger, Tahoe, and Ram/Powell fields, *in* Weimer, P., ed., Proceedings of the 20th Annual Research Conference: Houston, Texas, Gulf Coast Section, Society for Sedimentary Geology (SEPM), p. 450–468, https://doi.org/10.5724/gcs.00.15.0450.

Kindinger, J.L., 1989, Depositional history of the Lagniappe delta, northern Gulf of Mexico: Geo-Marine Letters, v. 9, p. 59–66, https://doi.org/10.1007/BF02430425.

Kluesner, J., Hart, P., Snyder, G., and Triezenberg, P., 2024, National Archive of Marine Seismic Surveys web portal provides public access to US Exclusive Economic Zone marine seismic surveys: Perspectives of Earth and Space Scientists, v. 5, https://doi.org/10.1029/2023CN000229.

Kneller, B., Dykstra, M., Fairweather, L., and Milana, J.P., 2016, Mass-transport and slope accommodation: Implications for turbidite sandstone reservoirs: American Association of Petroleum Geologists Bulletin, v. 100, p. 213–235, https://doi.org/10.1306/09011514210.

Kohl, B., Fillon, R.H., and Roberts, H.H., 2004, Foraminiferal biostratigraphy and paleoenvironments of the Pleistocene Lagniappe delta and related section, northeastern Gulf of Mexico, *in* Anderson, J.B., and Fillon, R., eds., Late Quaternary Stratigraphic Evolution of the Northern Gulf of Mexico Margin: Society for Sedimentary Geology (SEPM) Special Publication 79, p. 189–216, https://doi.org/10.2110/pec.04.79.0189.

Kolla, V., Biondi, P., Long, B., and Fillon, R., 2000, Sequence stratigraphy and architecture of the late Pleistocene Lagniappe delta complex, northeast Gulf of Mexico, *in* Hunt, D., and Gawthorpe, R.L., eds., Sedimentary Responses to Forced Regressions: Geological Society, London, Special Publication 172, p. 291–327, https://doi.org/10.1144/GSL.SP.2000.172.01.14.

Kolla, V., Fillon, R.H., Roberts, H.H., Kohl, B., and Long, B., 2003, Late Pleistocene sequence stratigraphy and architecture of the Late Pleistocene Lagniappe delta complex, northeast Gulf of Mexico, *in* Weimer, P., Bouma, A.H., and Perkins, B.F., eds., Submarine Fans and Turbidite Systems: Proceedings of the 15th Annual Research Conference: Houston, Texas, USA, Gulf Coast Section, Society for Sedimentary Geology (SEPM), p. 79–89.

Kostic, S., Parker, G., and Marr, J.G., 2002, Role of turbidity currents in setting the foreset slope of clinoforms prograding into standing fresh water: Journal of Sedimentary Research, v. 72, p. 353–362, https://doi.org/10.1306/081501720353.

Lisiecki, L.E., and Raymo, M.E., 2005, A Pliocene–Pleistocene stack of 57 globally distributed benthic $\delta^{18}O$ records: Paleoceanography, v. 20, https://doi.org/10.1029/2004PA001071.

Martin, J., Paola, C., Abreu, V., Neal, J., and Sheets, B., 2009, Sequence stratigraphy of experimental strata under known conditions of differential subsidence and variable base level: American Association of Petroleum Geologists Bulletin, v. 93, p. 503–533, https://doi.org/10.1306/12110808057.

Meckel, L.D., 2003, Shelf-margin deltas: The key to big reserves, *in* Roberts, N.C., Rosen, N.C., Fillon, R.F., and Anderson, J.B., eds., Shelf Margin Deltas and Linked Down Slope Petroleum Systems; Global Significance and Future Exploration Potential, 23rd Annual Research Conference: Houston, Texas, Gulf Coast Section, Society for Sedimentary Geology (SEPM), p. 167–204.

Meckel, T.A., Trevino, R., and Hovorka, S.D., 2017, Offshore CO_2 storage resource assessment of the northern Gulf of Mexico: Energy Procedia, v. 114, p. 4728–4734, https://doi.org/10.1016/j.egypro.2017.03.1609.

Miller, K.G., Mountain, G.S., Wright, J.D., and Browning, J.V., 2011, A 180-million-year record of sea level and ice volume variations from continental margin and deep-sea isotopic records: Oceanography (Washington, D.C.), v. 24, p. 40–53, https://doi.org/10.5670/oceanog.2011.26.

Mitchum, R.M., Vail, P.R., and Sangree, J.B., 1977, Seismic stratigraphy and global changes of sea level, part 6: Stratigraphic interpretation of seismic reflection patterns in depositional sequences, *in* Payton, C.E., ed., Seismic Stratigraphy—Applications to Hydrocarbon Exploration: American Association of Petroleum Geologists Memoir 26, p. 117–133, https://doi.org/10.1306/M26490C8.

Mohrig, D., Heller, P.L., Paola, C., and Lyons, W.J., 2000, Interpreting avulsion process from ancient alluvial sequences: Guadalope-Matarranya system (northern Spain) and Wasatch Formation (western Colorado): Geological Society of America Bulletin, v. 112, p. 1787–1803, https://doi.org/10.1130/0016-7606(2000)112<1787:IAPFAA>2.0.CO;2.

Moscardelli, L., and Wood, L., 2016, Morphometry of mass-transport deposits as a predictive tool: Geological Society of America Bulletin, v. 128, p. 47–80, https://doi.org/10.1130/B31221.1.

Nienhuis, J.H., Ashton, A.D., and Giosan, L., 2015, What makes a delta wave-dominated?: Geology, v. 43, p. 511–514, https://doi.org/10.1130/G36518.1.

Nienhuis, J.H., Ashton, A.D., Edmonds, D.A., Hoitink, A.J.F., Kettner, A.J., Rowland, J.C., and Törnqvist, T.E., 2020, Global-scale human impact on delta morphology has led to net land area gain: Nature, v. 577, p. 514–518, https://doi.org/10.1038/s41586-019-1905-9.

Normark, W.R., Posamentier, H., and Mutti, E., 1993, Turbidite systems: State of the art and future directions: Reviews of Geophysics, v. 31, p. 91–116, https://doi.org/10.1029/93RG02832.

Paumard, V., Bourget, J., Payenberg, T., George, A.D., Ainsworth, R.B., Lang, S., and Posamentier, H.W., 2020, Controls on deep-water sand delivery beyond the shelf edge: Accommodation, sediment supply, and deltaic process regime: Journal of Sedimentary Research, v. 90, p. 104–130, https://doi.org/10.2110/jsr.2020.2.

Portnov, A., Santra, M., Cook, A.E., and Sawyer, D.E., 2020, The Jackalope gas hydrate system in the northeastern Gulf of Mexico: Marine and Petroleum Geology, v. 111, p. 261–278, https://doi.org/10.1016/j.marpetgeo.2019.08.036.

Posamentier, H.W., and Kolla, V., 2003, Seismic geomorphology and stratigraphy of depositional elements in deep-water settings: Journal of Sedimentary Research, v. 73, p. 367–388, https://doi.org/10.1306/111302730367.

Pratson, L.F., and Coakley, B.J., 1996, A model for the headward erosion of submarine canyons induced by downslope-eroding sediment flows: Geological Society of America Bulletin, v. 108, p. 225–234, https://doi.org/10.1130/0016-7606(1996)108<0225:AMFTHE>2.3.CO;2.

Prior, D.B., and Suhayda, J.N., 1979, Application of infinite slope analysis to subaqueous sediment instability, Mississippi Delta: Engineering Geology, v. 14, p. 1–10. https://doi.org/10.1016/0013-7952(79)90059-0.

Roberts, H.H., Fillon, R.H., Kohl, B., Robalin, J.M., and Sydow, J.C., 2004, Depositional architecture of the Lagniappe delta: Sediment characteristics, timing of depositional events, and temporal relationship with adjacent shelf-edge deltas, *in* Anderson, J.B., and Fillon, R., eds., Late Quaternary Stratigraphic Evolution of the Northern Gulf of Mexico Margin: Society for Sedimentary Geology (SEPM) Special Publication 79, p. 143–188, https://doi.org/10.2110/pec.04.79.0143.

Romero-Otero, G.A., Slatt, R.M., and Pirmez, C., 2015, Evolution of the Magdalena deepwater fan in a tectonically active setting, offshore Colombia, *in* Bartolini, C., and Mann, P., eds., Petroleum Geology and Potential of the Colombian Caribbean Margin: American Association of Petroleum Geologists Memoir 108, p. 675–708, https://doi.org/10.1306/13531953M1083656.

Ross, W.C., Halliwell, B.A., May, J.A., Watts, D.E., and Syvitski, J.P.M., 1994, Slope readjustment: A new model for the development of submarine fans and aprons: Geology, v. 22, p. 511–514, https://doi.org/10.1130/0091-7613(1994)022<0511:SRANMF>2.3.CO;2.

Sheets, B.A., Hickson, T.A., and Paola, C., 2002, Assembling the stratigraphic record: Depositional patterns and time-scales in an experimental alluvial basin: Basin Research, v. 14, p. 287–301, https://doi.org/10.1046/j.1365-2117.2002.00185.x.

Shepard, F.P., 1955, Delta-front valleys bordering the Mississippi distributaries: Geological Society of America Bulletin, v. 66, p. 1489–1498, https://doi.org/10.1130/0016-7606(1955)66[1489:DVBTMD]2.0.CO;2.

Straub, K.M., 2019, Morphodynamics and stratigraphic architecture of shelf-edge deltas subject to constant vs. dynamic environmental forcings: A laboratory study: Frontiers of Earth Science, v. 7, https://doi.org/10.3389/feart.2019.00121.

Straub, K.M., and Mohrig, D., 2009, Constructional canyons built by sheet-like turbidity currents: Observations from offshore Brunei Darussalam: Journal of Sedimentary Research, v. 79, p. 24–39, https://doi.org/10.2110/jsr.2009.006.

Straub, K.M., and Pyles, D.R., 2012, Quantifying the hierarchical organization of compensation in submarine fans using surface statistics: Journal of Sedimentary Research, v. 82, p. 889–898, https://doi.org/10.2110/jsr.2012.73.

Straub, K.M., Paola, C., Mohrig, D., Wolinsky, M.A., and George, T., 2009, Compensational stacking of channelized sedimentary deposits: Journal of Sedimentary Research, v. 79, p. 673–688, https://doi.org/10.2110/jsr.2009.070.

Straub, K.M., Mohrig, D., and Pirmez, C., 2012, Architecture of an aggradational tributary submarine-channel network on the continental slope offshore Brunei Darussalam, *in* Prather, B.E., Deptuck, M.E., Mohrig, D., Van Hoorn, B., and Wynn, R.B., eds., Application of the Principles of Seismic Geomorphology to Continental Slope and Base-of-Slope Systems: Case Studies from SeaFloor and Near-Sea Floor Analogues: Society for Sedimentary Geology (SEPM) Special Publication 99, p. 13–30, https://doi.org/10.2110/pec.12.99.0013.

Strong, N., and Paola, C., 2008, Valleys that never were: Time surfaces versus stratigraphic surfaces: Journal of Sedimentary Research, v. 78, p. 579–593, https://doi.org/10.2110/jsr.2008.059.

Suter, J.R., and Berryhill, H.L., Jr., 1985, Late Quaternary shelf-margin deltas, northwest Gulf of Mexico: American Association of Petroleum Geologists Bulletin, v. 69, p. 77–91, https://doi.org/10.1306/AD461B92-16F7-11D7-8645000102C1865D.

Sydow, J., and Roberts, H.H., 1994, Stratigraphic framework of a late Pleistocene shelf-edge delta, northeast Gulf of Mexico: American Association of Petroleum Geologists Bulletin, v. 78, p. 1276–1312, https://doi.org/10.1306/A25FEAD1-171B-11D7-8645000102C1865D.

Sylvester, Z., Deptuck, M.E., Prather, B.E., Pirmez, C., and O'Byrne, C., 2012, Seismic stratigraphy of a shelf-edge delta and linked submarine channels in the northeastern Gulf of Mexico, *in* Prather, B.E., Deptuck, M.E., Mohrig, D., Van Hoorn, B., and Wynn, R.B., eds., Application of the Principles of Seismic Geomorphology to Continental Slope and Base-of-Slope Systems: Case Studies from SeaFloor and Near-Sea Floor Analogues: Society for Sedimentary Geology (SEPM) Special Publication 99, p. 31–59, https://doi.org/10.2110/pec.12.99.0031.

Sylvester, Z., Straub, K.M., and Covault, J.A., 2024, Stratigraphy in space and time: A reproducible approach to analysis and visualization: Earth-Science Reviews, v. 250, https://doi.org/10.1016/j.earscirev.2024.104706.

Triezenberg, P.J., Hart, P.E., and Childs, J.R., 2016, National Archive of Marine Seismic Surveys (NAMSS): A USGS data website of marine seismic reflection data within the U.S. Exclusive Economic Zone (EEZ): U.S. Geological Survey Data Release, https://doi.org/10.5066/F7930R7P.

Wallace, K.J., Meckel, T.A., Carr, D.L., Treviño, R.H., and Yang, C., 2014, Regional CO_2 sequestration capacity assessment for the coastal and offshore Texas Miocene interval: Greenhouse Gases: Science and Technology, v. 4, no. 1, p. 53–65, https://doi.org/10.1002/ghg.1380.

Willis, B., and Sun, T., 2019, Relating depositional processes of river-dominated deltas to reservoir behavior using computational stratigraphy: Journal of Sedimentary Research, v. 89, p. 1250–1276, https://doi.org/10.2110/jsr.2019.59.

Willis, B.J., Sun, T., and Ainsworth, R.B., 2021, Contrasting facies patterns between river-dominated and symmetrical wave-dominated delta deposits: Journal of Sedimentary Research, v. 91, p. 262–295, https://doi.org/10.2110/jsr.2020.131.

Winker, C.D., 1982, Cenozoic shelf margins, northwestern Gulf of Mexico: Transactions of the Gulf Coast Association of Geological Societies, v. 32, p. 427–448.

Winker, C.D., 1993, Leveed slope channels and shelf-margin deltas of the late Pliocene to middle Pleistocene Mobile River, NE Gulf of Mexico: Comparison with sequence-stratigraphic models [abs.], *in* American Association of Petroleum Geologists Annual Convention Program, New Orleans: American Association of Petroleum Geologists, p. 201.

Winker, C.D., and Edwards, M.B., 1983, Unstable progradational clastic shelf margins, *in* Stanley, D.J., and Moore, G.T., eds., The Shelfbreak: Critical Interface on Continental Margins: Society for Sedimentary Geology (SEPM) Special Publication 33, p. 139–157, https://doi.org/10.2110/pec.83.06.0139.

Wright, L.D., 1985, River deltas, *in* Davis, R.A., ed., Coastal Sedimentary Environments: New York, Springer, p. 1–76, https://doi.org/10.1007/978-1-4612-5078-4_1.